

NASA Technical Paper 1043

Effects of Control Inputs
on the Estimation of Stability
and Control Parameters
of a Light Airplane

LOAN COPY: RETURN TO
AFWL TECHNICAL LIBRARY
KIRTLAND AFB, NM

0134265



Robert L. Cannaday and William T. Suit

DECEMBER 1977

NASA



NASA Technical Paper 1043

Effects of Control Inputs
on the Estimation of Stability
and Control Parameters
of a Light Airplane

Robert L. Cannaday and William T. Suit
Langley Research Center
Hampton, Virginia



National Aeronautics
and Space Administration

**Scientific and Technical
Information Office**

1977

SUMMARY

The maximum likelihood parameter estimation technique was used to extract values of stability and control derivatives from flight test data obtained from a light, single-engine, low-wing airplane. The flight tests consisted of 9 runs in which the stabilator was used to excite the longitudinal motions and 28 runs in which the rudder and ailerons were used to excite lateral motions. The various control inputs were initiated from trimmed level flight with a trimmed air-speed of about 46 m/sec and an initial altitude of about 600 m.

The consistency of the derivative estimates as it relates to various inputs was investigated to determine the inputs which provide the most information for identification. Three criteria were used in this investigation: the ensemble variance, the estimated Cramér-Rao lower bound, and parameter correlations. There were no significant differences in the consistencies obtained by using the various stabilator inputs. On the other hand, for the lateral case, the sequential inputs (rudder followed by ailerons or ailerons followed by rudder) gave noticeable improvement in parameter value consistency over the rudder or aileron inputs individually. Also, some improvement in consistency was noted for both aileron and rudder square waves as opposed to sine waves.

The derivative values obtained by using the maximum likelihood technique were compared with values computed by using an empirical approach. They compared favorably in direct comparison and in comparison of time histories of computed airplane motions, although the extracted parameters provided the better match.

INTRODUCTION

The maximum likelihood technique (ref. 1) has been used to estimate values of the aerodynamic derivatives for several airplanes ranging from experimental high-performance airplanes (refs. 2 and 3) to single-engine light airplanes (ref. 4). The importance of proper inputs to the success of the parameter identification process has long been recognized (ref. 5), and several input design studies have been conducted using modern control theory (refs. 5 to 8). The inputs developed in these studies can be difficult to implement in practice, and approximations of these optimal inputs are often used. The approach taken in this paper to determine the effectiveness of inputs in parameter identification was to perform repeatedly several different inputs which were roughly based on some of these designed inputs (refs. 6 to 8). The resulting parameter estimates for each type of input were compared to indicate how well the inputs provided the information required to define each parameter precisely.

The purpose of this paper is to present the evaluation of the effectiveness of different inputs in providing consistent parameter estimates. This was done by conducting flight tests using several types of inputs, extracting parameters

from the flight test records, and using three criteria to determine the relative effectiveness of the various inputs relating to parameter estimation. The three criteria used for input evaluation in the study were to compare (1) the variances of the estimated parameter values, (2) the estimates of the Cramér-Rao lower bound (ref. 9), and (3) the parameter correlations.

This report first describes the airplane, instrumentation, and flight tests. Then the control inputs used in the tests are described and the three criteria used for comparing these inputs are discussed briefly. The results of these comparisons are presented next. Finally, a comparison of the parameter estimates with those computed by using an empirical-theoretical approach is presented.

SYMBOLS

The aerodynamic parameters are referenced to a system of body axes with the origin at the airplane center of gravity, which is located at 21.25 percent \bar{c} , and with orientation of body axes as shown in figure 1.

a_x, a_y, a_z	acceleration measured along X, Y, and Z body axis, respectively, g units
b	wing span, m
\bar{c}	wing mean geometric chord, m
F_x, F_y, F_z	force along X, Y, and Z body axis, respectively, N
g	acceleration due to gravity, m/sec ²
I_x, I_y, I_z	moment of inertia about X, Y, and Z body axis, respectively, kg-m ²
I_{xz}	product of inertia, kg-m ²
i	index
J	cost function
L	likelihood function
l_t	distance from airplane center of gravity to center of pressure of horizontal tail, m
M_x, M_y, M_z	rolling, pitching, and yawing moments, respectively, N-m
m	mass, kg
N	number of data points
n	dimension of system
2	

p	roll rate, rad/sec
p'	number of parameters to be identified
q	pitch rate, rad/sec
\bar{q}	dynamic pressure, N/m^2
R_1	estimate of error covariance matrix
r	yaw rate, rad/sec
S	wing area, m^2
s	standard deviation
$s\sigma_{CRLB}$	standard deviation of estimated Cramér-Rao lower bound
T	thrust, N
u, v, w	velocity along X, Y, and Z body axis, respectively, m/sec
u', v', w'	velocity component along X, Y, and Z body axis, respectively, at angle-of-attack sensor on wing-tip boom, m/sec
V	airplane total velocity, m/sec
X, Y, Z	body coordinate axes through airplane center of gravity
x, y, z	body coordinates, m
$\bar{x}, \bar{y}, \bar{z}$	x-, y-, and z-coordinates, respectively, of the sensors on wing-tip boom relative to airplane center of gravity, m
\vec{x}	vector describing state of airplane
α	angle of attack, rad
\vec{d}	parameter vector
$\vec{\Delta\alpha}$	parameter change vector
β	angle of sideslip, rad
δ_a	left aileron deflection minus right aileron deflection, rad
δ_e	stabilator deflection, rad
δ_r	rudder deflection, rad
$(\delta_a)_{si}$	aileron sine-wave input

$(\delta_a)_{sq}$	aileron square-wave input	
$(\delta_e)_{pul}$	stabilator rapid pulse followed by slower decay	
$(\delta_e)_{si}$	stabilator sine-wave input	
$(\delta_e)_{sq}$	stabilator square-wave input	
$(\delta_r)_{si}$	rudder sine-wave input	
$(\delta_r)_{sq}$	rudder square-wave input	
$(\delta_a-\delta_r)_{si}$	aileron sine-wave input followed by rudder sine-wave input	
$(\delta_a-\delta_r)_{sq}$	aileron square-wave input followed by rudder square-wave input	
$(\delta_r-\delta_a)_{si}$	rudder sine-wave input followed by aileron sine-wave input	
$(\delta_r-\delta_a)_{sq}$	rudder square-wave input followed by aileron square-wave input	
ϵ	angle between thrust axis and airplane X body axis, positive for thrust up, rad	
$\vec{\eta}$	measurement noise vector ($n \times 1$)	
θ	pitch angle, rad	
ρ	air density, kg/m^3	
$\bar{\sigma}_{CRLB}$	ensemble mean estimated Cramér-Rao lower bound	
ϕ	roll angle, rad	
C_l	rolling-moment coefficient, $M_X/\bar{q}Sb$	
C_m	pitching-moment coefficient, $M_Y/\bar{q}S\bar{c}$	
C_n	yawing-moment coefficient, $M_Z/\bar{q}Sb$	
C_T	thrust coefficient, $T/\bar{q}S$ (used in some publications as T_c')	
C_X	axial-force coefficient, $F_X/\bar{q}S$	
C_Y	side-force coefficient, $F_Y/\bar{q}S$	
C_Z	normal-force coefficient, $F_Z/\bar{q}S$	
$C_{lp} = \frac{\partial C_l}{\partial \frac{pb}{2V}}$	$C_{lr} = \frac{\partial C_l}{\partial \frac{rb}{2V}}$	$C_{l\beta} = \frac{\partial C_l}{\partial \beta}$

$$C_{1\delta a} = \frac{\partial C_1}{\partial \delta_a}$$

$$C_{1\delta r} = \frac{\partial C_1}{\partial \delta_r}$$

$$C_{mq} = \frac{\partial C_m}{\partial \frac{q\bar{c}}{2V}}$$

$$C_{m\alpha} = \frac{\partial C_m}{\partial \alpha}$$

$$C_{m\dot{\alpha}} = \frac{\partial C_m}{\partial \frac{\dot{\alpha}\bar{c}}{2V}}$$

$$C_{m\delta e} = \frac{\partial C_m}{\partial \delta_e}$$

$$C_{np} = \frac{\partial C_n}{\partial \frac{pb}{2V}}$$

$$C_{nr} = \frac{\partial C_n}{\partial \frac{rb}{2V}}$$

$$C_{n\beta} = \frac{\partial C_n}{\partial \beta}$$

$$C_{n\delta a} = \frac{\partial C_n}{\partial \delta_a}$$

$$C_{n\delta r} = \frac{\partial C_n}{\partial \delta_r}$$

$$C_{T\alpha} = \frac{\partial C_T}{\partial \alpha}$$

$$C_{X\alpha} = \frac{\partial C_X}{\partial \alpha}$$

$$C'_{X\alpha} = C_{X\alpha} + C_{T\alpha} \cos \epsilon$$

$$C_{Yp} = \frac{\partial C_Y}{\partial \frac{pb}{2V}}$$

$$C_{Yr} = \frac{\partial C_Y}{\partial \frac{rb}{2V}}$$

$$C_{Y\beta} = \frac{\partial C_Y}{\partial \beta}$$

$$C_{Y\delta r} = \frac{\partial C_Y}{\partial \delta_r}$$

$$C_{Zq} = \frac{\partial C_Z}{\partial \frac{q\bar{c}}{2V}}$$

$$C_{Z\alpha} = \frac{\partial C_Z}{\partial \alpha}$$

$$C'_{Z\alpha} = C_{Z\alpha} + C_{T\alpha} \sin \epsilon$$

$$C_{Z\delta e} = \frac{\partial C_Z}{\partial \delta_e}$$

Subscripts:

- c computed
- k index
- m measured
- o coefficient at trimmed conditions
- t trimmed conditions

Superscripts:

- T transpose matrix
- M measured quantity
- o nominal evaluation

A dot over a symbol signifies a derivative with respect to time.

DESCRIPTION OF AIRPLANE, INSTRUMENTATION, FLIGHT TESTS,
AND DATA REDUCTION

The subject airplane for this study was a four-place, low-wing, single-engine airplane shown in figure 2. Its pertinent geometric details are given in table I. The movable control surfaces included the stabilator, rudder, ailerons, and flaps; and the airplane was instrumented to record control-surface movements and airplane responses to these movements.

The variables recorded for this study were obtained from an onboard instrumentation package. The range of each instrument used to record the pertinent variables is given in table II. The accelerations, angular rates, and angular attitudes were recorded continuously, whereas the airspeed, angle of attack, angle of sideslip, and control-surface positions were recorded sequentially by use of a commutator which sampled each variable 20 times per second. Airspeed, angle of attack, and angle of sideslip were measured on a boom that was located near the wing tip and extended $3/4 \bar{c}$ ahead of the wing leading edge. (See fig. 2.)

The flight tests were divided into two groups: those in which the longitudinal modes were excited and those in which the lateral modes were excited. No flaps were used during the flight tests and all tests were initiated from trimmed level flight. The test procedure was as follows: The pilot turned on the data recording equipment, made specific control inputs, allowed airplane responses to settle out, and then turned off the recording equipment. This sequence constituted a data run. The tests were conducted in smooth air to minimize process noise from gusts. The throttle was held fixed during the runs to minimize any changes in thrust so that the only disturbing force on the airplane was due to the control input. Since angle-of-attack oscillations during the tests were generally less than 7° peak to peak, these variations were considered minimal, although the reader should note possible thrust change effects on $C_{X\alpha}$ and $C_{Z\alpha}$ as stated in appendix A.

A total of 37 flight test runs were made, 9 runs concentrating on longitudinal dynamics and the remainder concentrating on lateral dynamics. The length of the runs ranged from about 20 to 50 sec. Since the object of the flight test was to evaluate the relative effectiveness of various inputs for parameter estimation, all test runs were initiated from approximately the same condition of trimmed level flight. The flight condition was between approach and cruise airspeed (approximately 40 percent power). For the longitudinal tests, the mean initial trimmed airspeed was 45.3 m/sec with a standard deviation of 1.7 m/sec and the initial altitude was 641 m with a standard deviation of 57 m. For the lateral tests, the mean initial trimmed airspeed was 45.8 m/sec with a standard deviation of 1.6 m/sec, and the initial altitude was 564 m with a standard deviation of 24 m. Effects of variations in airspeed and altitude were considered to be negligible and were ignored in the processing and analysis of the data.

It was necessary to apply corrections to some of the data before processing with the identification algorithm. Airspeed was corrected for position error and altitude (assuming standard temperature) to obtain true airspeed. Then airspeed, angle of attack, and angle of sideslip were corrected for upwash and

resolved into velocity components u , v , and w by using the relationships developed in appendix B. The control-surface positions were measured at the respective cables in the vicinity of the cockpit. Because some of the data were commutated, it was necessary to reconstruct the data between data points by linear interpolation and then sample simultaneously to avoid time-shift errors due to commutation. The continuous data were sampled digitally by using a zero-phase Ormsby filter (ref. 10).

The accelerometers were considered to be located on the airplane center of gravity in the X-Y plane but their z-position relative to the airplane center of gravity was unknown. The computer program used for identification had the option of identifying the z-position of the Y-accelerometer; so this variable was activated in the algorithm for the appropriate maneuvers. Therefore, the accelerometer data were not corrected to the center-of-gravity position before being examined by use of the identification algorithm. A brief description of the identification algorithm is contained in appendix C.

CONTROL INPUTS

Various control inputs were used to determine dependence of parameter consistency on the inputs. Some of the inputs were suggested by several input design studies (refs. 6, 7, and 8) and others were inputs common to flight testing. The inputs used in this study were not the optimal inputs of these studies but were simplified forms.

For the identification of the longitudinal parameters, three basic types of inputs were attempted: the stabilator square wave, sine wave, and rapid rise followed by slower decay. The square-wave input (input A, fig. 3) was chosen because it was thought to contain the frequency content necessary to excite the short-period mode. The period and amplitude (stabilator travel) were chosen for ease of pilot implementation, as well as to keep pitch-attitude changes within 5° to 10° of trim. The stabilator sine-wave input (input B, fig. 3) is often used to characterize a second-order system. The stabilator rapid rise followed by slower decay (input C, fig. 3) was an attempt to approximate an input form suggested by reference 6.

For lateral identification, inputs consisted of rudder or ailerons applied individually or a sequential combination of both. (See fig. 4.) Switching-type (square-wave) inputs were recommended in several references (for example, refs. 7 and 8) as an approximation to the optimal input; therefore, square-wave inputs were attempted, although the switching times and amplitudes used for the tests were not optimal. Both sine- and square-wave forms were investigated for each control. The resulting inputs were rudder square wave (input D), rudder sine wave (input E), aileron square wave (input F), and aileron sine wave (input G).

Rudder inputs alone do not provide adequate excitation of the lateral modes for parameter identification (ref. 11). To provide better excitation than single controls (rudder or ailerons individually) can produce, combinations of rudder and ailerons were used sequentially. That is, the aileron inputs were implemented followed immediately by rudder inputs or rudder inputs were followed by aileron inputs. The resulting sequential inputs were rudder square wave fol-

lowed by aileron square wave (input H), rudder sine wave followed by aileron sine wave (input I), aileron square wave followed by rudder square wave (input J), and aileron sine wave followed by rudder sine wave (input K). Typical time histories of these inputs can be seen in figure 4.

Several repeat runs were made for each input in an effort to obtain the desired input form. Inspection of the data for each input form showed that none of the input repeats excelled over the others, so all the runs were used for analysis. For the longitudinal inputs, this resulted in five repeats of input A and two of B and C. For the lateral inputs, D and E each had four repeats, F had two, G had four, H had five, I had three, J had four, and K had two.

CRITERIA USED FOR EVALUATING INPUTS

The results from each of the several different control inputs were examined before presenting a set of stability and control derivative values which best described the subject airplane. In determining which inputs provided the most consistent identification of the parameter values, three criteria were considered: ensemble variance of the parameter estimates, estimated Cramér-Rao lower bound (ref. 9), and parameter correlations.

The ensemble variance is the variance of the parameter estimates from the same type of input. These variances of the parameter estimates were compared by using the F-tests (ref. 12). This comparison indicated which inputs produced the most consistent identification of the unknown parameters.

The next criterion, the estimated Cramer-Rao lower bound, was examined also using the F-test for further indication of the effectiveness of the inputs for identification. According to reference 9, the estimated Cramér-Rao lower bound is proportional to the uncertainty level in the estimate of an unknown parameter. The primary function of these uncertainty levels used here was to indicate which inputs provided the greatest information and, inversely, the least uncertainty in defining a particular derivative value. The higher the uncertainty level for a particular derivative, the less information was generated by the input to define that derivative. Therefore, a comparison of the uncertainty levels obtained for a parameter from various inputs gave some indication of which inputs provided the best identification of that parameter.

Another criterion that aids in discerning which inputs provide the more reliable identification of the unknown parameters is the correlations, or dependencies, between pairs of parameters (ref. 6). These correlations between parameters are determined from the off-diagonal terms of the error covariance matrix for estimated parameters (parameter covariance matrix). Correlation values near ± 1 indicate parameter dependencies, that is, changes in one parameter value causing changes in another. These parameter dependencies do not necessarily arise from physical relationships, but may also arise from inadequate excitation of some of the states for which parameters are to be identified. Inadequate excitation can be analogous to the problem of attempting to identify too many parameters (ref. 6). High correlations can result in a nonuniqueness of the identification problem which can result in parameter ratios or sums of parameters being identified rather than the specific parameters themselves. Although reliable

parameter estimates can occur even when correlations are high, in many cases non-realistic parameter values and significant run-to-run scatter have occurred when correlation coefficients are 0.9 or larger. Therefore, large correlation coefficients are an indication of potential identification problems. One way these parameter dependencies can be reduced is by choosing inputs that adequately excite the modes for which the associated parameters are to be identified. Therefore, examination of the parameter covariance matrix associated with each input revealed which input reduced parameter dependencies or correlations and, in turn, probably provided the more reliable parameter estimates.

RESULTS AND DISCUSSION

In order to evaluate the uniformity of input repeats, the mean input period and amplitude and the associated standard deviations for each input are presented in table III. As can be noted, there was considerable variability in the mean period among the lateral inputs (5.4 to 10.4 sec). Generally, this variability did not appear to correspond to the scatter in the parameter estimates.

Effects of Various Longitudinal Control Inputs

The longitudinal parameter values obtained from applying the maximum likelihood technique to the longitudinal flight test data are presented in figure 5 and table IV. In the upper half of figure 5 are the longitudinal parameter values obtained for each run for inputs A, B, and C. Note that the run numbers are located beside the extracted values and, in some cases, the extracted values overlap so closely that one symbol may represent two or three data points. In the lower half of figure 5 are the mean values for each type of input, with the upper and lower bars representing plus and minus values of the standard deviation for each parameter. Also, just to the right of these bars are bars representing the mean plus or minus the mean of the estimated Cramér-Rao lower bound for each input.

Comparing the variances (F-test) of the longitudinal parameter estimates across the inputs indicated no significant differences. Therefore, based on the variance criterion, none of the stabilator inputs showed significant improvement in providing consistent estimates of the parameters.

The next criterion to be considered was the uncertainty level (based on the estimated Cramér-Rao lower bound) in the parameter estimates. A visual inspection of figure 5 shows little difference in longitudinal parameter uncertainty levels among the inputs. The F-test was applied to the square of the uncertainty levels of the parameter estimates for the three inputs. Based on uncertainty levels, none of the longitudinal inputs stood out as significantly improving the consistency of the parameter estimates. This same conclusion was reached by considering the variance, so the conclusions for these two criteria are consistent.

The third criterion, the parameter correlations, was considered next. For the present study, basically the only longitudinal parameters which appeared to be correlated were $C_{m\dot{q}}$ and $C_{m\delta_e}$. For input A, the correlation between these

two parameters ranged from 0.90 to 0.95; for input B, from 0.93 to 0.96; and for input C, from 0.84 to 0.91. Also, for input B, run 6 exhibited relatively high correlations for some of the other parameters also. Based on parameter correlations, input C appeared to offer slightly improved identification. The form of input C was loosely patterned after the optimal input of reference 6, which was based on criteria related to the trace and determinant of the Fisher information matrix. This matrix is the inverse of the parameter covariance matrix.

Based on the three criteria considered, none of the three longitudinal inputs clearly offered better identification than the other two.

Effects of Various Lateral Control Inputs

The lateral parameter values obtained from the flight data are shown in figure 6 and table V. The lateral data are presented in the same format as that used for the longitudinal data. Note that no attempt was made to identify aileron control derivatives with rudder inputs or rudder control derivatives with aileron inputs.

A visual inspection of the data reveals that inputs with rudder alone (D and E) generally gave the least consistent estimates of the parameters except for the rudder control derivatives. Correspondingly, ailerons alone (inputs F and G) generally provided more consistent estimates than the rudder alone. For one of the aileron runs (run 22 of input G), however, the parameter estimates were considerably out of line for the rolling- and yawing-moment parameters. An examination of the time history of run 22 showed that the period of the input was about 2 sec longer than the other runs for input G, although the basic form was the same. This long input period may not have properly excited the airplane dynamics and thus may have resulted in some identification problems. Parameter correlations for run 22 were exceptionally high and are discussed subsequently. Due to the problems encountered with run 22, the associated parameter values were omitted from the computation of the statistics shown in the lower half of figure 6.

To investigate lateral inputs as they relate to consistent identification, the three criteria - ensemble variance, uncertainty level, and parameter correlations - were again used as for the longitudinal parameters.

In order to determine whether input form affected consistency, results from inputs D and E, and F and G were compared by using the variance criterion (F-test). For rudder input forms, D generally provided more consistent estimates than E but only $C_{Y\beta}$, $C_{Y\delta_r}$, and C_{n_r} were significantly more consistent (80-percent level). In no case did input E provide significantly greater consistency in the parameter estimates than input D. This result seems to indicate that, for rudder inputs, rudder square waves provided the better identification. For aileron inputs, F provided more consistent estimates than G (sine waves). Input F demonstrates significantly greater consistency for $C_{Y\beta}$, C_{Y_p} , $C_{l\beta}$, and $C_{n\delta_a}$ than input G. Therefore, it appears that square-wave inputs provided

the more consistent estimates for ailerons also, but uncertainty levels (estimated Cramér-Rao lower bound) and parameter correlations should be examined before a conclusion is drawn.

Rudder inputs were next compared to aileron inputs. Comparing rudder square-wave inputs (D) with aileron square-wave inputs (F) showed that for $C_{Y\beta}$, C_{Yp} , C_{Yr} , and $C_{l\beta}$, ailerons provided significantly (80-percent level).

more consistent identification and in no case did input D provide more consistent estimates than any of the runs using aileron inputs. A similar trend, although less pronounced, held when comparing inputs E and G (rudder and aileron sine waves), with C_{Yp} and $C_{n\beta}$ being significantly more consistently

identified for the aileron inputs. It is interesting to note that for single control inputs, the derivatives which might be assumed to be associated with excitations from the rudder inputs appear to be better defined by using aileron inputs. One explanation is that the correlations between parameters were higher for the rudder inputs, making identification of the correlated parameters difficult. Correlations are discussed in more detail subsequently.

Upon comparing the single control inputs (D, E, F, and G) with the sequential inputs (H, I, J, and K) it was found that the sequential inputs provided significantly more consistent estimates of most of the stability derivatives, with the exception of input F. Input F was nearly as consistent as the sequential inputs, but this may be due to the small data sample (2 runs). For the control derivatives, the single inputs generally provided estimates which were equally as consistent as those obtained with sequential inputs.

Inputs H and J, and I and K were compared to determine whether the order of the inputs for the sequential inputs was significant. Input J gave significantly (80-percent level) more consistent estimates of the rolling-moment derivatives except for $C_{l\beta}$, and input H gave significantly more consistent estimates of C_{Yr} and $C_{Y\delta r}$. These trends did not hold when comparing inputs I and K; only $C_{Y\delta r}$ was identified as significantly more consistent and this was for input I. Therefore, based on the information examined thus far, it is difficult to conclude whether order makes any difference.

The next criterion to be considered in evaluating input effectiveness for identification purposes was the uncertainty level, or estimated Cramér-Rao lower bound. Generally, uncertainty levels were less than the standard deviations, especially for the single inputs (D, E, F, and G). Greater uncertainty levels in many cases corresponded to greater standard deviations, which indicated that uncertainty levels were somewhat analogous to standard deviations, as stated in reference 9. Therefore, the trends determined by using the F-test on the variances should generally hold when considering the square of the uncertainty levels. Looking at input form (comparing data from inputs D and E, and F and G) the distinction between parameter estimates that was noted when comparing ensemble variance was not as obvious when comparing the square of the uncertainty level. Statistically speaking, none of the estimated parameters had signifi-

Error

An error occurred while processing this page. See the system log for more details.

and $C_{l\delta a}$ with coefficient values ranging from 0.85 to 0.89 and $C_{n\dot{p}}$ and $C_{n\delta a}$ with values ranging from 0.815 to 0.869. Inputs I and K were not quite as effective in reducing correlations as H and J but were considerably more effective than D, E, F, and G.

Based on the information contained in the parameter covariance matrix, the sequential inputs clearly reduce parameter correlations, or dependencies, compared to the single control inputs. This implies that the more reliable lateral identification is obtained from the sequential inputs.

The z-position of the Y-accelerometer was also identified for the lateral runs. As for the parameter estimates, the most consistent estimate of the location was observed for the sequential inputs. These estimates ranged from 0.24 to 0.30 m below the airplane center of gravity.

Use of Estimated Parameters in Mathematical Model

None of the longitudinal inputs attempted offered clear improvement in the consistency of the extracted derivatives. Therefore, the resulting parameters presented for the subject airplane are the arithmetic means of the various parameter values extracted for all 9 longitudinal runs. These mean values along with standard deviations are presented in table VI.

For the lateral data, the sequential inputs generally provided the most consistent estimates of the lateral parameters. Therefore, the arithmetic means of the parameters obtained from the sequential inputs were used to describe the airplane in the subsequent analysis. These mean values are also presented in table VI.

The mean parameter values of table VI were used to generate the computed time histories of figures 7 and 8. The match between the computed airplane responses and the measured responses was considered to be good, although a slightly better fit could be obtained with the actual values for that run.

The last column in table VI contains the standard deviations as a percent of the mean value for each derivative. This quantity, the coefficient of variation, provides a measure of the relative consistency of one derivative with another. For example, $C_{n\dot{\beta}}$ (3.6 percent) was the most consistent lateral derivative identified and $C_{Z\alpha}$ (4.0 percent) was the most consistent longitudinal derivative. Generally, the static derivatives such as $C_{Z\alpha}$ and $C_{n\dot{\beta}}$ were more consistently identified than were the rotational and control derivatives.

Comparison of the Extracted Parameters

One question which arises whenever derivatives are extracted from flight data is, Are the results reasonable? Good agreement between measured and com-

puted time histories does not necessarily guarantee that the parameters are reasonable. Correlations, an inadequate mathematical model, or other problems could exist which could drive the parameters to unrealistic values to fit the data. Therefore, to lend some confidence to the extracted parameter values, these values were compared with results for the same airplane, which were determined by another method. The second column of table VII contains the estimated parameter values given in table VI. The third column of table VII contains an estimate of the stability and control derivatives of the subject airplane obtained by using the theoretical-empirical techniques presented in reference 13. These values were transformed to body-axis derivatives by the transformations presented in reference 14. Upon comparison, it can be seen that the estimated parameter values of the present study are generally consistent with those computed from reference 13.

As a matter of interest, the derivative values obtained by using the maximum likelihood technique, as well as those from reference 13, were used in the equations of motion to generate time histories. The computed time histories based on the derivative values and the accelerometer offset obtained by using the maximum likelihood technique and the measured flight data time histories are shown in figures 7 and 8. The computed time histories based on the derivatives obtained by using the methods of reference 13 and the same accelerometer offset and the same flight data time histories are shown in figures 9 and 10. As would be expected, the maximum likelihood derivatives provided the better fit to the flight data, which was especially noticeable for the lateral data.

CONCLUDING REMARKS

Stability and control derivative values were determined by use of the maximum likelihood algorithm from flight test data taken in cruise conditions for a low-wing, single-engine airplane. Various control inputs were used to determine whether certain inputs improved the run-to-run consistency of the derivative estimates. The longitudinal inputs included stabilator square waves and sine waves and a rapid rise followed by a slower decay. The lateral inputs consisted of rudder and aileron inputs (square and sine waves) individually and in sequence.

The parameter values obtained from the various inputs were compared for improved consistency by using three criteria: the ensemble variance of the parameter estimates, the estimated Cramér-Rao lower bound, and parameter correlations. The results indicated that none of the longitudinal inputs resulted in improved identification. On the other hand, the lateral inputs which consisted of rudder and ailerons in sequence clearly offered improved consistency over the rudder or aileron inputs individually.

For the single inputs, the square-wave inputs for both rudder and ailerons generally provided the more consistent parameter estimates when compared with their sine-wave counterparts. For the sequential inputs, square-wave inputs appeared to provide more precise estimates of the parameters. The order of the sequential inputs made little difference in the consistency of the estimates.

In order to validate the parameter values determined by use of the maximum likelihood algorithm, parameter values for the subject airplane were also determined by a theoretical-empirical method. These values and those obtained by using the maximum likelihood algorithm were compared both individually and in their ability to describe the airplane dynamics accurately. The results indicated that the values from the maximum likelihood algorithm more nearly described the airplane motions.

Langley Research Center
National Aeronautics and Space Administration
Hampton, VA 23665
November 17, 1977

APPENDIX A

EQUATIONS OF MOTION

The equations used in this program are perturbation equations from trimmed level flight and are written relative to the set of body axes shown in figure 1.

The equations used to describe the longitudinal motions were

$$\dot{u} = -qw + rv - g \sin \theta + \frac{1}{2} \rho \frac{V^2 S}{m} [C_{X,o} + C'_{X\alpha} (\alpha - \alpha_t)] \quad (A1)$$

$$\begin{aligned} \dot{w} = & -\rho v + qu + g \cos \theta \cos \phi + \frac{1}{2} \rho \frac{V^2 S}{m} [C_{Z,o} + C'_{Z\alpha} (\alpha - \alpha_t) + C_{Zq} \frac{q\bar{c}}{2V} \\ & + C_{Z\delta_e} (\delta_e - \delta_{e,t})] \end{aligned} \quad (A2)$$

$$\begin{aligned} \dot{q} = & pr \frac{I_X - I_Y}{I_Y} + \frac{I_{XZ}(r^2 - p^2)}{I_Y} + \rho \frac{V^2 S \bar{c}}{2I_Y} [C_{m,o} + C_{m\alpha} (\alpha - \alpha_t) + C_{m\dot{\alpha}} \frac{\dot{\alpha}\bar{c}}{2V} \\ & + C_{mq} \frac{q\bar{c}}{2V} + C_{m\delta_e} (\delta_e - \delta_{e,t})] \end{aligned} \quad (A3)$$

$$\dot{\theta} = q \cos \phi - r \sin \phi \quad (A4)$$

$$a_X = \frac{1}{g} (\dot{u} + qw - rv + g \sin \theta) \quad (A5)$$

$$a_Z = \frac{1}{g} (\dot{w} + pv - qu - g \cos \theta \cos \phi) \quad (A6)$$

$$V = \sqrt{u^2 + v^2 + w^2} \quad (A7)$$

$$\alpha = \tan^{-1} \frac{w}{u} \quad (A8)$$

$$\dot{\alpha} \approx \frac{\dot{w}}{u} \quad (A9)$$

$$C_{Z\delta_e} = \frac{\bar{c}}{l_t} C_{m\delta_e} \quad (A10)$$

APPENDIX A

The values of the lateral states v , p , r , and ϕ used in the longitudinal equations were the flight-measured quantities.

Since thrust changes are not explicitly modeled in the equations of motion, $C'_{X\alpha}$ of equation (A1) and $C'_{Z\alpha}$ of equation (A2) are not necessarily pure $C_{X\alpha}$ and $C_{Z\alpha}$ but may contain small contributions due to changes in thrust. Therefore, $C'_{X\alpha}$ and $C'_{Z\alpha}$, as determined in this study, are given by

$$C'_{X\alpha} = \frac{\partial C_X}{\partial \alpha} + C_{T\alpha} \cos \epsilon$$

$$C'_{Z\alpha} = \frac{\partial C_Z}{\partial \alpha} + C_{T\alpha} \sin \epsilon$$

Since, in this study, thrust was held constant and the angle-of-attack changes were no more than 7° peak to peak, the contributions of thrust to $C'_{X\alpha}$ and $C'_{Z\alpha}$ were considered minimal.

The equations used to compute the lateral motions were

$$\begin{aligned} \dot{v} = & -ru + pw + g \cos \theta \sin \phi + \frac{1}{2} \rho \frac{V^2 S}{m} \left[C_{Y,o} + C_{Y\beta} \beta + C_{Y_r} \frac{rb}{2V} \right. \\ & \left. + C_{Y_p} \frac{pb}{2V} + C_{Y_{\delta r}} (\delta_r - \delta_{r,t}) \right] \end{aligned} \quad (A11)$$

$$\begin{aligned} \dot{p} = & \frac{I_{XZ}}{I_X} \dot{r} + \left(\frac{I_Y - I_Z}{I_X} \right) qr + \left(\frac{I_{XZ}}{I_X} \right) pq + \frac{1}{2} \rho \frac{V^2 S b}{I_X} \left[C_{l,o} + C_{l\beta} \beta + C_{l_p} \frac{pb}{2V} \right. \\ & \left. + C_{l_r} \frac{rb}{2V} + C_{l_{\delta r}} (\delta_r - \delta_{r,t}) + C_{l_{\delta a}} (\delta_a - \delta_{a,t}) \right] \end{aligned} \quad (A12)$$

$$\begin{aligned} \dot{r} = & \frac{I_{XZ}}{I_Z} \dot{p} + \left(\frac{I_X - I_Y}{I_Z} \right) pq - \left(\frac{I_{XZ}}{I_Z} \right) qr + \frac{1}{2} \rho \frac{V^2 S b}{I_Z} \left[C_{n,o} + C_{n\beta} \beta + C_{n_p} \frac{pb}{2V} \right. \\ & \left. + C_{n_r} \frac{rb}{2V} + C_{n_{\delta r}} (\delta_r - \delta_{r,t}) + C_{n_{\delta a}} (\delta_a - \delta_{a,t}) \right] \end{aligned} \quad (A13)$$

$$\dot{\phi} = p + (q \sin \phi + r \cos \phi) \tan \theta \quad (A14)$$

$$a_Y = \frac{1}{g} (\dot{v} + ru - pw - g \cos \theta \sin \phi) \quad (A15)$$

APPENDIX A

$$V = \sqrt{u^2 + v^2 + w^2} \quad (\text{A16})$$

$$\beta = \sin^{-1} \frac{v}{V} \quad (\text{A17})$$

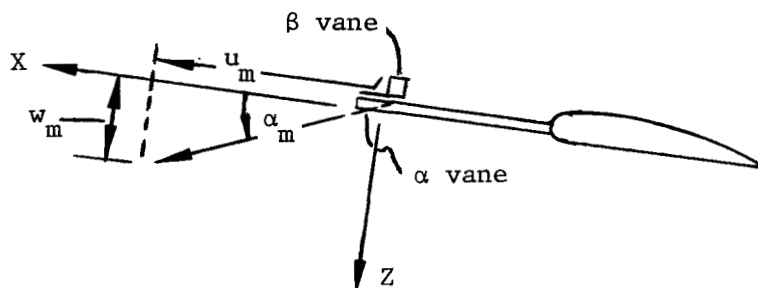
The values of longitudinal states u , w , q , and θ used in the lateral equations were the flight-measured quantities. The equations were used to compute the airplane state responses. The computed responses were then compared with the recorded responses from the flight tests and the differences were used to update the parameters (stability and control derivatives) to improve the fit.

The longitudinal measured and computed responses, or states, used in the algorithm for this study were u , w , q , θ , a_x , and a_z . The lateral states used were v , p , r , ϕ , and a_y . An abbreviated discussion of the identification algorithm is given in appendix C.

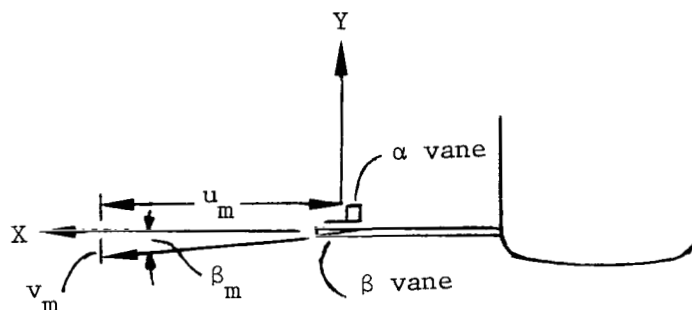
APPENDIX B

TRANSFORMATION OF MEASURED V , α , AND β

The boom on which the dynamic pressure, angle of attack, and angle of sideslip were measured was located at the left wing tip parallel to the airplane X body axis. The sensing elements were located about $3/4 \bar{c}$ ahead of the leading edge of the wing. These measurements were corrected for upwash and transformed to the airplane center-of-gravity position. The following development describes the procedure used for the data of this study. The following sketches show the side view



and the top view



of the schematic of the left wing tip. The equations related to these sketches are

$$u_m = V_m \cos \alpha_m$$

$$w_m = V_m \sin \alpha_m$$

$$w_m = u_m \tan \alpha_m \tag{B1}$$

$$v_m = u_m \tan \beta_m \tag{B2}$$

The magnitude of the velocity vector was measured by the pitot static tube and the direction was given by the α and β vanes. The magnitude of the velocity vector is given by the equation

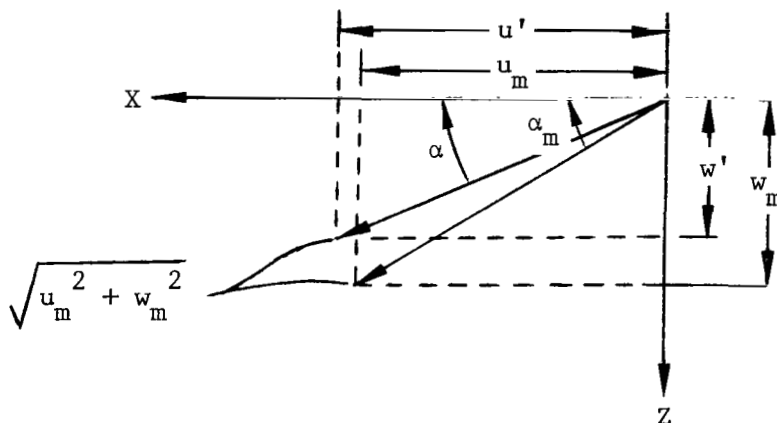
APPENDIX B

$$V_m = \sqrt{u_m^2 + v_m^2 + w_m^2} \quad (B3)$$

Substituting equations (B1) and (B2) into equation (B3) gives

$$u_m = \frac{V_m}{\sqrt{1 + \tan^2 \beta_m + \tan^2 \alpha_m}} \quad (B4)$$

It was assumed that the v-component was unaffected by the upwash and needed no upwash correction. Therefore, the problem was considered to be contained in the X-Z plane as shown in the following sketch:



As can be seen from this sketch, in order to correct velocity components u_m and w_m for upwash, the affected velocity vector needs to be rotated an amount which will result in u' and w' being the correct components when the rotated vector is projected onto the X- and Z-axes.

Based on experimental data, the angle of attack corrected for upwash α was determined to be $0.75\alpha_m$; that is, $\alpha = 0.75\alpha_m$. Therefore,

$$u' = \sqrt{u_m^2 + w_m^2} \cos (0.75\alpha_m)$$

$$v' = v_m$$

$$w' = \sqrt{u_m^2 + w_m^2} \sin (0.75\alpha_m)$$

Substitution of equations (B1), (B2), and (B4) into these equations yields

$$u' = \frac{V_m \sqrt{1 + \tan^2 \alpha_m} \cos (0.75\alpha_m)}{\sqrt{1 + \tan^2 \beta_m + \tan^2 \alpha_m}}$$

$$v' = \frac{V_m \tan \beta_m}{\sqrt{1 + \tan^2 \beta_m + \tan^2 \alpha_m}}$$

APPENDIX B

$$w' = \frac{V_m \sqrt{1 + \tan^2 \alpha_m} \sin (0.75\alpha_m)}{\sqrt{1 + \tan^2 \beta_m + \tan^2 \alpha_m}}$$

The components u' , v' , and w' are the upwash corrected components of velocity at the boom. These components must also be corrected to the airplane center-of-gravity position by removing velocities resulting from rotational rates about the center of gravity. This correction results in the following equations:

$$u = u_m \cos (0.75\alpha_m) - q\bar{z} + r\bar{y} \quad (B5)$$

$$v = u_m \tan \beta_m - r\bar{x} + p\bar{z} \quad (B6)$$

$$w = u_m \sin (0.75\alpha_m) - p\bar{y} + q\bar{x} \quad (B7)$$

where \bar{x} , \bar{y} , and \bar{z} denote the position of the sensors relative to the airplane center of gravity.

APPENDIX C

PARAMETER ESTIMATION PROCEDURE

The parameter estimation procedure used in this study is known as the maximum likelihood technique. This formulation of the maximum likelihood technique considered only measurement noise. The technique utilizes the differences between the measured and computed states (fit error) to estimate the unknown values of the parameters necessary to minimize the fit error. The measurement noise

$$\vec{\eta}(t_i) = \vec{x}^M(t_i) - \vec{x}_c(\vec{\alpha}, t_i)$$

is assumed to be white with Gaussian distribution. This assumption is used to construct the likelihood function, the natural logarithm of which is

$$\ln L(\vec{\alpha}^0, R_1) = -\frac{1}{2} \sum_{i=1}^N \vec{\eta}^T(t_i) R_1^{-1} \vec{\eta}(t_i) - \frac{N}{2} \ln |R_1|$$

where R_1 is the estimate of the state error covariance matrix based on the nominal solution, t_i is time, and $\vec{\alpha}^0$ is the nominal parameter vector.

To estimate the parameter vector $\vec{\alpha}$ the likelihood function was maximized with respect to $\vec{\alpha}^0$ and R_1 . Because of the nonlinear nature of the estimation problem, it was necessary to use an iterative procedure to estimate the parameters. Therefore, $\vec{x}(\vec{\alpha}, t_i)$, the estimated state vector at time t_i , was expanded about the nominal parameter vector, neglecting second-order and higher order terms. That is,

$$\vec{x}(\vec{\alpha}^0 + \Delta\vec{\alpha}, t_i) = \vec{x}(\vec{\alpha}^0, t_i) + \sum_{j=1}^{p'} \left(\frac{\partial \vec{x}(t_i)}{\partial \alpha_j} \right)^0 \Delta\alpha_j$$

expresses the estimated state vector as a function of the nominal solution plus the change in the state vector estimate as a function of the computed change in the parameter vector. This expression for the state vector estimation is then used in the fit error vector to obtain

$$\vec{\eta}(t_i) \approx \vec{x}^M(t_i) - \vec{x}^0(t_i) - A(t_i)^0 \Delta\vec{\alpha} = \vec{\eta}(t_i)^0 - A(t_i)^0 \Delta\vec{\alpha}$$

where

$$A(t_i)^0 = \sum_{j=1}^{p'} \left(\frac{\partial \vec{x}(t_i)}{\partial \alpha_j} \right)^0$$

and defines state sensitivity to the current parameters. Therefore, the natural logarithm of the likelihood function becomes

APPENDIX C

$$\ln L(\vec{\alpha}^0 + \vec{\Delta\alpha}, R_1) \approx -\frac{1}{2} \sum_{i=1}^N \left\{ \left[\vec{\eta}(t_i) - A(t_i)\vec{\Delta\alpha} \right]^T R_1^{-1} \left[\vec{\eta}(t_i) - A(t_i)\vec{\Delta\alpha} \right] \right\} - \frac{N}{2} \ln |R_1|$$

Maximizing the likelihood function with respect to $\vec{\Delta\alpha}$,

$$\frac{\partial \ln L(\vec{\alpha}^0 + \vec{\Delta\alpha}, R_1)}{\partial \vec{\Delta\alpha}} = 0$$

and solving for $\vec{\Delta\alpha}$ yield the parameter change equations,

$$\vec{\Delta\alpha} = \left[\sum_{i=1}^N A^T(t_i) R_1^{-1} A(t_i) \right]^{-1} \left[\sum_{i=1}^N A^T(t_i) R_1^{-1} \vec{\eta}(t_i) \right]$$

which are used to compute the $\vec{\Delta\alpha}$ that tends to maximize the likelihood function. Note that the matrix $\left[\sum_{i=1}^N A^T(t_i) R_1^{-1} A(t_i) \right]^{-1}$ is the estimate of the error covariance matrix for the estimated parameters (parameter covariance matrix). This matrix contains the parameter dependencies or correlations which are used to construct parameter correlation coefficients.

To estimate R_1 , the measurement noise covariance matrix, the likelihood function can be maximized with respect to R_1 , which is approximately

$$R_1 = \frac{1}{N} \sum_{i=1}^N \vec{\eta}(t_i) \vec{\eta}^T(t_i)$$

according to reference 1.

The effect of maximizing the likelihood function is the same as minimizing the cost function

$$J = \det \left\{ \frac{1}{N} \sum_{i=1}^N \vec{\eta}(t_i) \vec{\eta}^T(t_i) \right\}$$

In using the program, the cost function was computed and displayed on the program operator console (ref. 4). Generally, with each iteration the fit improved, as evidenced by a reduction in the cost function. Once the cost function settled out so that changes from iteration to iteration, as defined by $(J_k - J_{k+1})/J_k$, were less than 0.01, the parameters which maximize the likelihood function or minimize the cost function (fit error) were considered identified. The expression $(J_k - J_{k+1})/J_k$ represents the change in the fit error from successive iterations divided by the fit error of the previous iteration. To avoid possible correlation problems (see section "Criteria Used for Evaluating Inputs") between $C_{m\dot{\alpha}}$ and C_{mq} , $C_{m\dot{\alpha}}$ was held fixed at -4.00 (estimated in a preliminary study by using ref. 13), so essentially the program was identifying the combination $C_{mq} + C_{m\dot{\alpha}}$ with $C_{m\dot{\alpha}}$ held constant.

APPENDIX C

Also, to further reduce correlation problems between estimated parameters, $C_{Z\delta_e}$ and $C_{m\delta_e}$ were assumed to be geometrically related as

$$C_{Z\delta_e} = \frac{\bar{c}}{l_t} C_{m\delta_e}$$

as was done in reference 4. The program described in reference 1 was modified so that $C_{Z\delta_e}$ was not treated as an active parameter. Then $C_{m\delta_e}$ was extracted, and $C_{Z\delta_e}$ was calculated for each iteration and its value was substituted into the equations of motion. Although $C_{Z\delta_e}$ was not active, its value was changing from iteration to iteration. To account for this variation in $C_{Z\delta_e}$ in the sensitivity equations, $\frac{\bar{c}}{l_t} C_{m\delta_e}$ was substituted for $C_{Z\delta_e}$ in the \dot{w} equations and then the partial derivatives were taken of the \dot{w} equation with respect to $C_{m\delta_e}$ and $C_{Z\delta_e}$.

REFERENCES

1. Grove, Randall D.; Bowles, Roland L.; and Mayhew, Stanley C.: A Procedure for Estimating Stability and Control Parameters From Flight Test Data by Using Maximum Likelihood Methods Employing a Real-Time Digital System. NASA TN D-6735, 1972.
2. Williams, James L.; and Suit, William T.: Extraction From Flight Data of Lateral Aerodynamic Coefficients for F-8 Aircraft With Supercritical Wing. NASA TN D-7749, 1974.
3. Suit, William T.; and Williams, James L.: Lateral Static and Dynamic Aerodynamic Parameters of the Kestrel Aircraft (XV-6A) Extracted From Flight Data. NASA TN D-7455, 1974.
4. Suit, William T.: Aerodynamic Parameters of the Navion Airplane Extracted From Flight Data. NASA TN D-6643, 1972.
5. Mehra, R. K.; and Gupta, N. K.: Status of Input Design for Aircraft Parameter Identification. Methods for Aircraft State and Parameter Identification, AGARD-CP-172, May 1975, pp. 12-1 - 12-21.
6. Stepner, David E.; and Mehra, Raman K.: Maximum Likelihood Identification and Optimal Input Design for Identifying Aircraft Stability and Control Derivatives. NASA CR-2200, 1973.
7. Gupta, Narendra K.; and Hall, W. Earl, Jr.: Input Design for Identification of Aircraft Stability and Control Derivatives. NASA CR-2493, 1975.
8. Reid, Donald B.: Optimal Inputs for System Identification. SUDAAR No. 440 (NASA Grants NGR 05-020-526 and NGL 05-020-007), Stanford Univ., May 1972. (Available as NASA CR-128173.)
9. Iliff, Kenneth W.; and Maine, Richard E.: Practical Aspects of Using a Maximum Likelihood Estimation Method To Extract Stability and Control Derivatives From Flight Data. NASA TN D-8209, 1976.
10. Enochson, Loren D.; and Otnes, Robert K.: Programming and Analysis for Digital Time Series Data. SVM-3, U.S. Navy, 1968. (Available from DDC as AD 692 735.)
11. Klein, V.: Parameter Identification Applied to Aircraft. Cranfield Rep. Aero No. 26, Cranfield Inst. Technol., [Dec. 1974].
12. Ullman, Neil R.: Statistics - An Applied Approach. Xerox College Pub., c.1972.
13. Smetana, Frederick O.; Summey, Delbert C.; and Johnson, W. Donald: Riding and Handling Qualities of Light Aircraft - A Review and Analysis. NASA CR-1975, 1972.
14. Etkin, Bernard: Dynamics of Flight. John Wiley & Sons, Inc., c.1959.

TABLE I.- GEOMETRIC DETAILS OF SUBJECT AIRPLANE

Mass, kg	1074.1
Inertia:	
I_X , kg-m ²	1220
I_Y , kg-m ²	1898
I_Z , kg-m ²	2712
I_{XZ} , kg-m ²	68
Fuselage length, m	6.9
Wing:	
Area, m ²	14.9
Aspect ratio	5.625
Span, m	9.1
Mean geometric chord, m	1.62
Vertical tail:	
Area, m ²	1.07
Aspect ratio	2.02
Span, m	1.47
Rudder area, m ²	0.38
Horizontal tail (stabilator):	
Area, m ²	2.32
Aspect ratio	4.0
Span, m	3.05
Tail length, center of gravity to quarter-chord point of mean geometric chord, m	4.2
Location relative to airplane center of gravity of sensors to measure velocity, angle of attack, and angle of sideslip:	
\bar{x} , m	1.29
\bar{y} , m	-4.46
\bar{z} , m	0

TABLE II.- INSTRUMENTATION RANGES

Instrument function	Range
Airspeed, m/sec	0 to 61
Angle of attack, deg	-30 to 100
Angle of sideslip, deg	-60 to 60
Altitude, m	0 to 3050
Normal acceleration, g units	-3 to 6
Longitudinal acceleration, g units	-1 to 1
Lateral acceleration, g units	-1 to 1
Elevator position, deg	Full throw (1.5 to -19.0)
Aileron position, deg	Full throw (-43 to 43)
Rudder position, deg	Full throw (-25 to 25)
Throttle position	Full throw
Engine speed, rpm	0 to 2700
Pitch rate, deg/sec	-100 to 100
Roll rate, deg/sec	-180 to 180
Yaw rate, deg/sec	-180 to 180
Pitch attitude, deg	-85 to 85
Roll attitude, deg	-180 to 180

TABLE III.- CONSISTENCY OF INPUTS USED IN FLIGHT TEST

Input	Control	Input form (a)	Mean period, sec	Standard deviation of mean period, sec	Mean peak-to-peak amplitude, deg	Standard deviation of mean amplitude, deg
A	Stabilator	Square wave	4.2	0.6	2.4	0.4
B	Stabilator	Sine wave	5.5	1.0	2.5	.4
C	Stabilator	Rapid rise, slow decline each direction	4.4	.8	4.8	.4
D	Rudder	Square wave	5.5	.7	11.2	1.0
E	Rudder	Sine wave	6.6	1.2	20.8	2.8
F	Ailerons	Square wave	5.9	.6	^b 15.5	2.1
G	Ailerons	Sine wave	8.0	1.1	^b 15.8	1.5
H	Rudder and ailerons	Rudder square wave followed by aileron square wave	5.4	.5	10.0	1.0
			5.9	.6	^b 17.1	2.2
I	Rudder and ailerons	Rudder sine wave followed by aileron sine wave	7.9	.8	15.7	2.9
			8.1	1.2	^b 13.0	2.6
J	Ailerons and rudder	Aileron square wave followed by rudder square wave	5.8	.5	^b 15.3	1.7
			6.0	.4	12.4	1.5
K	Ailerons and rudder	Aileron sine wave followed by rudder sine wave	8.8	1.1	^b 15.1	1.3
			10.4	.8	17.5	3.5

^aInputs were not strictly sine waves or square waves but were pilot attempts at these forms. See figures 3 and 4 for typical input time histories.

^bAileron deflections are defined as left aileron minus right aileron.

TABLE IV.- ENSEMBLE MEAN AND STANDARD DEVIATION FOR EACH LONGITUDINAL
INPUT ALONG WITH ESTIMATED CRAMER-RAO LOWER BOUND

Parameter	Mean value	Standard deviation of mean value	$\bar{\sigma}_{\text{CRLB}}$	$s\sigma_{\text{CRLB}}$
Input A (5 runs)				
$C_{X,o}$	0.0533	0.0068	0.00022	0.00010
$C_{X\alpha}$.6481	.2275	.01830	.00735
$C_{Z,o}$	-.5533	.0465	.00060	.00029
$C_{Z\alpha}$	-4.3828	.1864	.03826	.00947
C_{Zq}	-15.1932	4.1709	.80940	.22418
$C_{m\alpha}$	-.4394	.0324	.00356	.00148
C_{mq}	-8.7746	3.7690	.20806	.09952
$C_{m\delta e}$	-1.5265	.2125	.01830	.00870
Input B (2 runs)				
$C_{X,o}$	0.0405	0.0156	0.00013	0.00007
$C_{X\alpha}$.7424	.1573	.00815	.00233
$C_{Z,o}$	-.5829	.0573	.00046	.00024
$C_{Z\alpha}$	-4.2332	.0433	.02680	.00424
C_{Zq}	-20.9335	1.0257	.59945	.06074
$C_{m\alpha}$	-.4723	.0071	.00260	.00057
C_{mq}	-7.6263	2.6367	.16445	.01407
$C_{m\delta e}$	-1.5265	.2850	.01560	.00042

TABLE IV.- Concluded

Parameter	Mean value	Standard deviation of mean value	$\bar{\sigma}_{\text{CRLB}}$	$s\sigma_{\text{CRLB}}$
Input C (2 runs)				
$C_{X,o}$	0.0469	0.0052	0.00020	0.00006
$C_{X\alpha}$.5076	.1623	.02120	.01018
$C_{Z,o}$	-.5644	.0508	.00054	.00009
$C_{Z\alpha}$	-4.4514	.2157	.04105	.00615
C_{Zq}	-17.0211	5.2584	.72725	.04632
$C_{m\alpha}$	-.4925	.0311	.00390	.00028
C_{mq}	-8.4654	1.1422	.16715	.04674
$C_{m\delta e}$	-1.5786	.0947	.01500	.00311

TABLE V.- ENSEMBLE MEAN AND STANDARD DEVIATION FOR EACH LATERAL INPUT
ALONG WITH ESTIMATED CRAMÉR-RAO LOWER BOUND.

(a) Input D (4 runs)

Parameter	Mean value	Standard deviation of mean value	$\bar{\sigma}_{\text{CRLB}}$	$s_{\sigma_{\text{CRLB}}}$
$C_{Y\beta}$	-0.5737	0.0799	0.0372	0.0229
C_{Yp}	-.0291	.5170	.2723	.1737
C_{Yr}	.2806	.2652	.0730	.0105
$C_{Y\delta r}$.0342	.0090	.0040	.0007
$C_{l\beta}$	-.0631	.0229	.0030	.0021
C_{lp}	-.3400	.1375	.0179	.0127
C_{lr}	.0376	.0475	.0060	.0034
$C_{l\delta r}$.0029	.0038	.0006	.0002
$C_{l\delta a}$	-----	-----	-----	-----
$C_{n\beta}$.0521	.0098	.0018	.0008
C_{np}	-.0480	.0619	.0107	.0045
C_{nr}	-.0923	.0212	.0034	.0012
$C_{n\delta r}$	-.0338	.0021	.0003	.00004
$C_{n\delta a}$	-----	-----	-----	-----

TABLE V.- Continued

(b) Input E (4 runs)

Parameter	Mean value	Standard deviation of mean value	$\bar{\sigma}_{\text{CRLB}}$	$s_{\sigma_{\text{CRLB}}}$
$C_{Y\beta}$	-0.4639	0.1868	0.0332	0.0100
C_{Yp}	.8892	1.0266	.1879	.0625
C_{Yr}	.7896	.2648	.1408	.0083
$C_{Y\delta r}$.0764	.0210	.0074	.0008
$C_{l\beta}$	-.0438	.0174	.0024	.0008
C_{lp}	-.2110	.0907	.0132	.0057
C_{lr}	.0647	.0526	.0076	.0034
$C_{l\delta r}$.0068	.0018	.0007	.0003
$C_{l\delta a}$	-----	-----	-----	-----
$C_{n\beta}$.0492	.0203	.0023	.0006
C_{np}	-.0802	.1216	.0130	.0038
C_{nr}	-.1042	.0502	.0052	.0024
$C_{n\delta r}$	-.0368	.0014	.0004	.0002
$C_{n\delta a}$	-----	-----	-----	-----

TABLE V.- Continued

(c) Input F (2 runs)

Parameter	Mean value	Standard deviation of mean value	$\bar{\sigma}_{\text{CRLB}}$	$s\sigma_{\text{CRLB}}$
$C_{Y\beta}$	-0.5396	0.0001	0.0061	0.0008
C_{Yp}	.0947	.0079	.0162	.0012
C_{Yr}	.3182	.0339	.0265	.0031
$C_{Y\delta r}$	-----	-----	-----	-----
$C_{l\beta}$	-.0413	.0010	.0012	.0003
C_{lp}	-.2538	.0262	.0081	.0001
C_{lr}	.0479	.0245	.0043	.0018
$C_{l\delta r}$	-----	-----	-----	-----
$C_{l\delta a}$	-.0390	.0018	.0009	.0001
$C_{n\beta}$.0598	.0038	.0004	.0008
C_{np}	-.0462	.0101	.0037	.0014
C_{nr}	-.1072	.0145	.0022	.0004
$C_{n\delta r}$	-----	-----	-----	-----
$C_{n\delta a}$.0058	.0002	.0004	.0001

TABLE V.- Continued

(d) Input G (3 runs)

Parameter	Mean value	Standard deviation of mean value	$\bar{\sigma}_{\text{CRLB}}$	$s_{\sigma_{\text{CRLB}}}$
$C_{Y\beta}$	-0.5022	0.0882	0.0177	0.0070
C_{Yp}	.0328	.1789	.0432	.0178
C_{Yr}	.1250	.1167	.0500	.0137
$C_{Y\delta r}$	-----	-----	-----	-----
$C_{1\beta}$	-.0284	.0147	.0020	.0010
C_{1p}	-.1837	.0468	.0101	.0013
C_{1r}	.0071	.0473	.0046	.0020
$C_{1\delta r}$	-----	-----	-----	-----
$C_{1\delta a}$	-.0288	.0092	.0011	.0002
$C_{n\beta}$.0606	.0011	.0009	.0006
C_{np}	-.0232	.0107	.0064	.0033
C_{nr}	-.1008	.0169	.0032	.0008
$C_{n\delta r}$	-----	-----	-----	-----
$C_{n\delta a}$.0083	.0022	.0007	.0002

TABLE V.- Continued

(e) Input H (5 runs)

Parameter	Mean value	Standard deviation of mean value	$\bar{\sigma}_{\text{CRLB}}$	$s_{\sigma_{\text{CRLB}}}$
$C_{Y\beta}$	-0.5442	0.0109	0.0048	0.0009
C_{Yp}	.1132	.0348	.0152	.0030
C_{Yr}	.3515	.0315	.0280	.0045
$C_{Y\delta r}$.0307	.0022	.0042	.0007
$C_{l\beta}$	-.0475	.0016	.0012	.0002
C_{lp}	-.2374	.0128	.0056	.0011
C_{lr}	.0766	.0315	.0042	.0007
$C_{l\delta r}$.0081	.0031	.0008	.0001
$C_{l\delta a}$	-.0397	.0026	.0008	.0002
$C_{n\beta}$.0560	.0013	.0004	.0001
C_{np}	-.0347	.0046	.0021	.0005
C_{nr}	-.0938	.0118	.0016	.0003
$C_{n\delta r}$	-.0338	.0015	.0003	.0001
$C_{n\delta a}$.0068	.0012	.0068	.0012

TABLE V.- Continued

(f) Input I (3 runs)

Parameter	Mean value	Standard deviation of mean value	$\bar{\sigma}_{\text{CRLB}}$	$s\sigma_{\text{CRLB}}$
$C_{Y\beta}$	-0.5706	0.0233	0.0076	0.0007
C_{Yp}	.1786	.0274	.0242	.0033
C_{Yr}	.3741	.0902	.0396	.0054
$C_{Y\delta r}$.0566	.0179	.0060	.0006
$C_{1\beta}$	-.0408	.0040	.0016	.0002
C_{1p}	-.2245	.0125	.0074	.0020
C_{1r}	.0678	.0284	.0052	.0008
$C_{1\delta r}$.0032	.0046	.0009	.0002
$C_{1\delta a}$	-.0349	.0011	.0010	.0002
$C_{n\beta}$.0553	.0038	.0008	.0001
C_{np}	-.0737	.0071	.0043	.0006
C_{nr}	-.0911	.0169	.0023	.0003
$C_{n\delta r}$	-.0386	.0028	.0004	.0001
$C_{n\delta a}$.0018	.0031	.0006	.0001

TABLE V.- Continued

(g) Input J (4 runs)

Parameter	Mean value	Standard deviation of mean value	$\bar{\sigma}_{\text{CRLB}}$	$s\sigma_{\text{CRLB}}$
$C_{Y\beta}$	-0.5516	0.0091	0.0048	0.0004
C_{Yp}	.1015	.0174	.0163	.0019
C_{Yr}	.4296	.0781	.0273	.0024
$C_{Y\delta r}$.0457	.0126	.00372	.0004
$C_{l\beta}$	-.0451	.0018	.0010	.0002
C_{lp}	-.2464	.0031	.0048	.0008
C_{lr}	.0750	.0050	.0034	.0008
$C_{l\delta r}$.0049	.0013	.0006	.0001
$C_{l\delta a}$	-.0397	.0005	.0007	.0001
$C_{n\beta}$.0557	.0012	.0004	.00003
C_{np}	-.0485	.0058	.0023	.0002
C_{nr}	-.1045	.0054	.0016	.0002
$C_{n\delta r}$	-.0375	.0014	.0003	.0001
$C_{n\delta a}$.0056	.0009	.0003	.00002

TABLE V.- Concluded

(h) Input K (2 runs)

Parameter	Mean value	Standard deviation of mean value	$\bar{\sigma}_{\text{CRLB}}$	$s\sigma_{\text{CRLB}}$
$C_{Y\beta}$	-0.5868	0.0035	0.0078	0.0002
C_{Yp}	.1146	.0267	.0219	.0012
C_{Yr}	.2929	.0457	.0405	.0009
$C_{Y\delta r}$.0623	.0017	.0058	.0001
$C_{l\beta}$	-.0483	.0032	.0015	.0002
C_{lp}	-.2054	.0302	.0056	.0004
C_{lr}	.0520	.0056	.0049	.0007
$C_{l\delta r}$.0106	.0060	.0008	.0001
$C_{l\delta a}$	-.0364	.0025	.0009	.00002
$C_{n\beta}$.0566	.0008	.0006	.00001
C_{np}	-.0451	.0113	.0030	.0002
C_{nr}	-.0948	.0035	.0021	.0002
$C_{n\delta r}$	-.0380	.0013	.0004	.00001
$C_{n\delta a}$.0042	.0008	.0005	.00002

TABLE VI.- MAXIMUM LIKELIHOOD ESTIMATES OF STABILITY AND
CONTROL DERIVATIVE VALUES FOR SUBJECT AIRPLANE

Derivative	Sample mean, P	Sample standard deviation, s	Coefficient of variation, $s/P \times 100$
$C_{X\alpha}$	0.638	0.198	31.0
$C_{Z\alpha}$	-4.365	.173	4.0
C_{Zq}	-16.875	4.264	25.3
$C_{Z\delta e}$	-.594	.072	12.1
$C_{m\alpha}$	-.458	.035	7.6
$C_{m\dot{\alpha}}$	^a -4.000		
C_{mq}	-8.451	2.893	34.2
$C_{m\delta e}$	-1.538	.185	12.0
$C_{Y\beta}$	-.558	.020	3.6
C_{Yp}	.124	.039	31.4
C_{Yr}	.370	.073	19.6
$C_{Y\delta r}$.045	.016	34.6
$C_{l\beta}$	-.046	.004	7.9
C_{lp}	-.233	.018	8.0
C_{lr}	.071	.023	32.0
$C_{l\delta r}$.006	.004	62.3
$C_{l\delta a}$	-.038	.003	7.1
$C_{n\beta}$.056	.002	3.6
C_{np}	-.048	.016	32.8
C_{nr}	-.096	.011	11.6
$C_{n\delta r}$	-.036	.003	8.3
$C_{n\delta a}$.005	.002	40.0

^aHeld constant.

TABLE VII.- COMPARISON OF DERIVATIVES FROM THE PRESENT STUDY
WITH THOSE FROM METHODS OF REFERENCE 13

Derivative	Present study	Reference 13
$C_{X\alpha}$	0.638	0.285
$C_{Z\alpha}$	-4.365	-4.755
C_{Zq}	-16.875	-3.012
$C_{Z\delta e}$	-.594	-.535
$C_{m\alpha}$	-.458	-.549
$C_{m\dot{\alpha}}$	^a -4.000	-3.052
C_{mq}	-8.451	-6.539
$C_{m\delta e}$	-1.538	-1.323
$C_{Y\beta}$	-.558	-.285
C_{Yp}	.124	-.156
C_{Yr}	.370	.226
$C_{Y\delta r}$.045	.132
$C_{l\beta}$	-.046	-.216
C_{lp}	-.233	-.425
C_{lr}	.071	.174
$C_{l\delta r}$.006	.012
$C_{l\delta a}$	-.038	^b -.071
$C_{n\beta}$.056	.058
C_{np}	-.048	-.041
C_{nr}	-.096	-.097
$C_{n\delta r}$	-.036	-.049
$C_{n\delta a}$.005	^b .019

^aHeld constant.

^bThe derivatives $C_{l\delta a}$ and $C_{n\delta a}$ from this source were multiplied by -0.5 to make them compatible with the conventions used in present study.

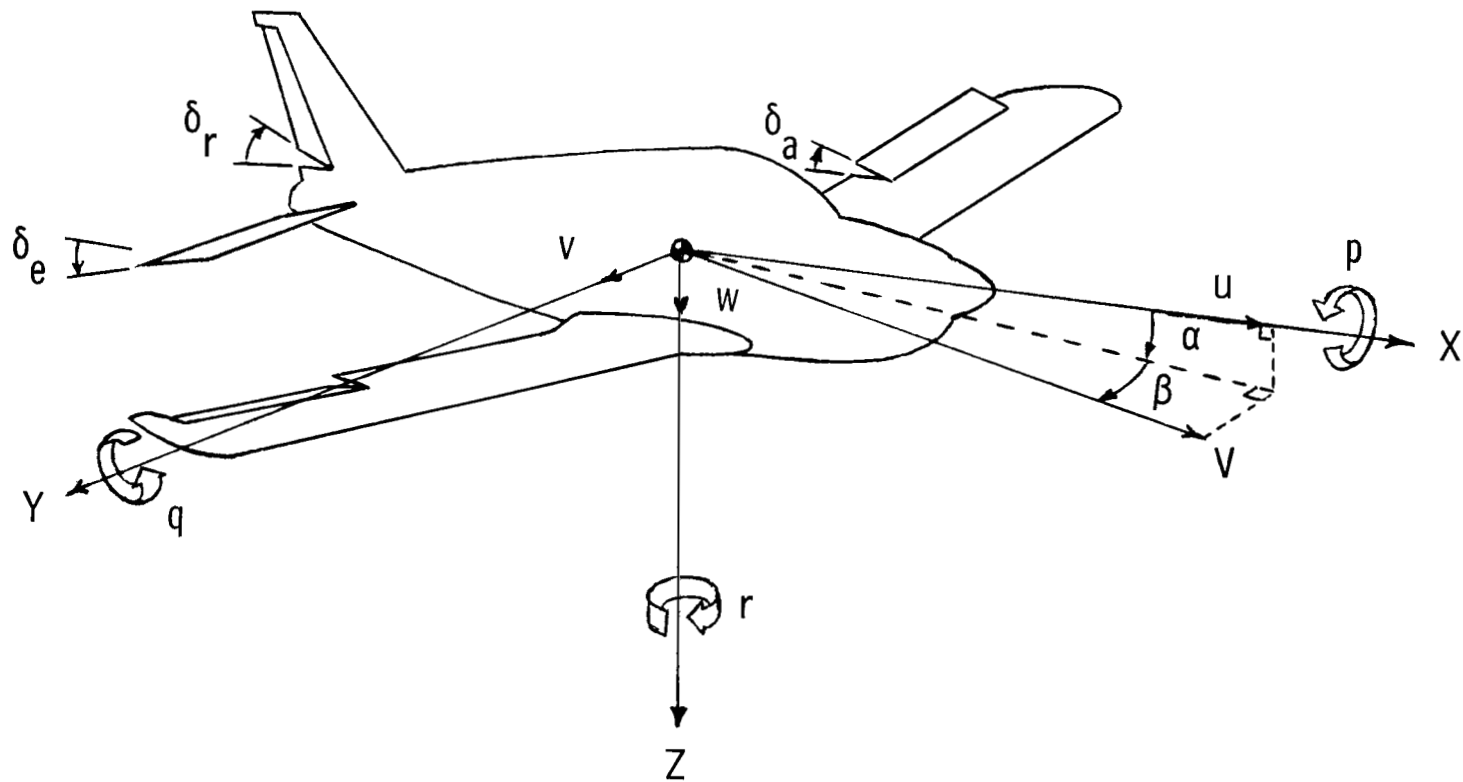


Figure 1.- System of body axes showing positive sense of velocities, forces, and control deflections.

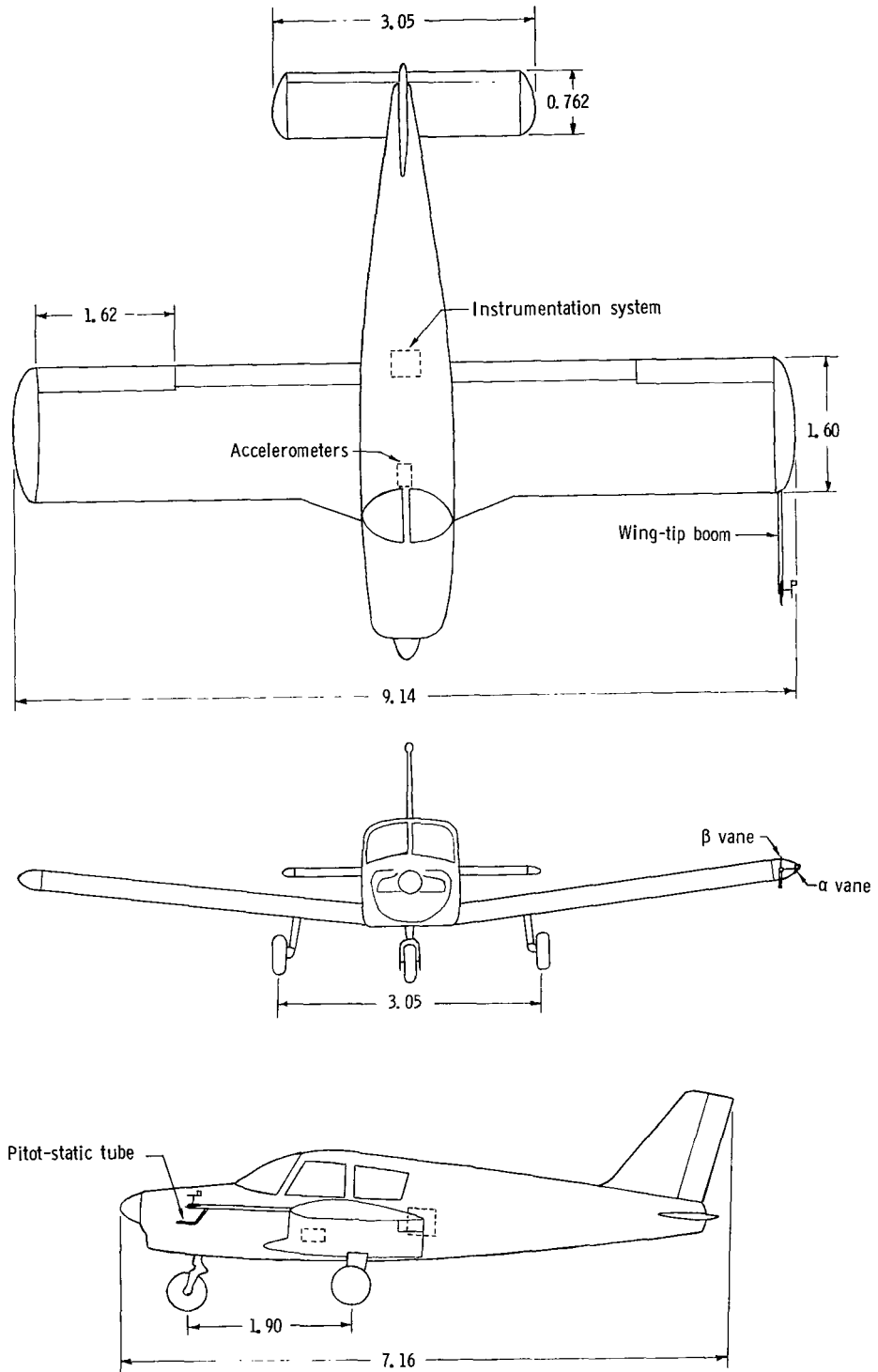


Figure 2.- Three-view drawing of subject airplane. All dimensions are in meters.

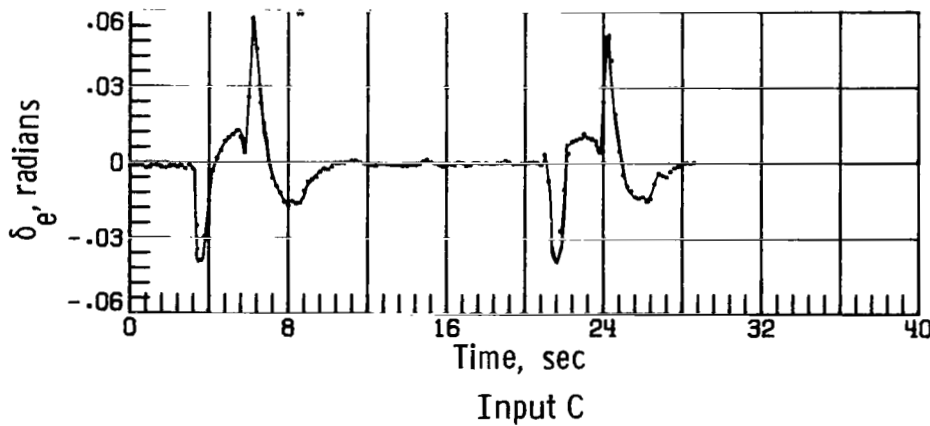
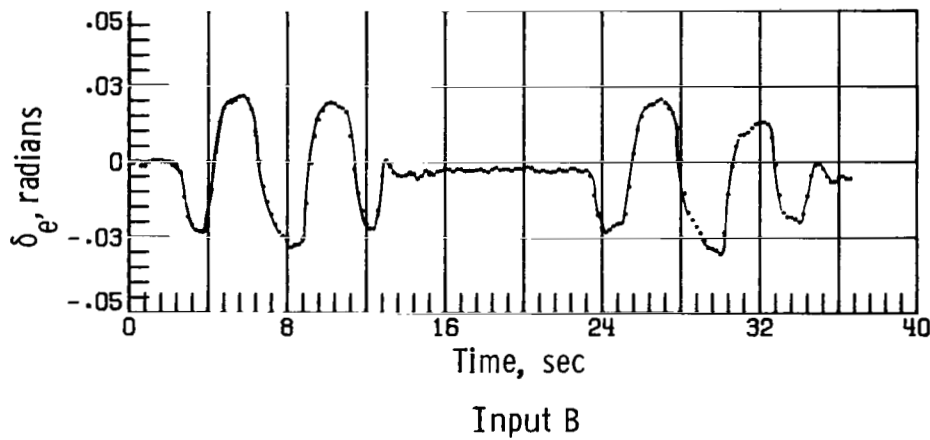
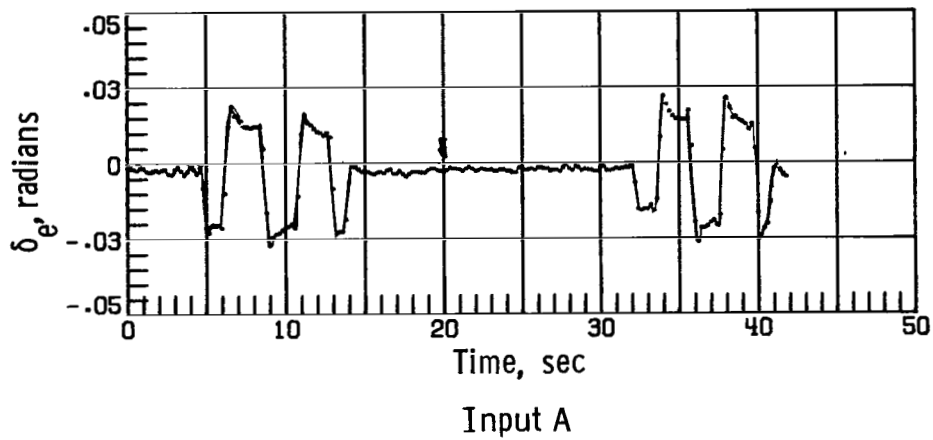
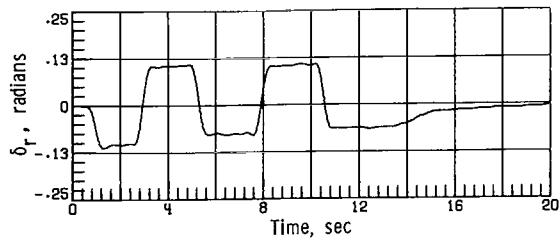
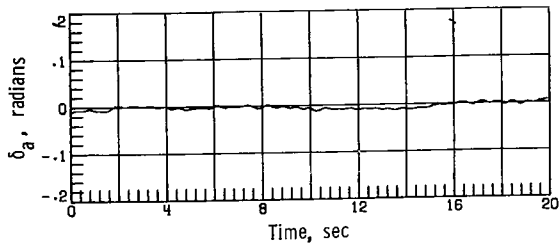
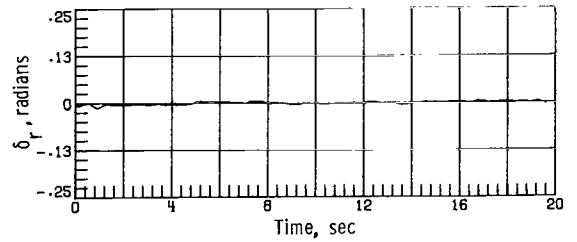
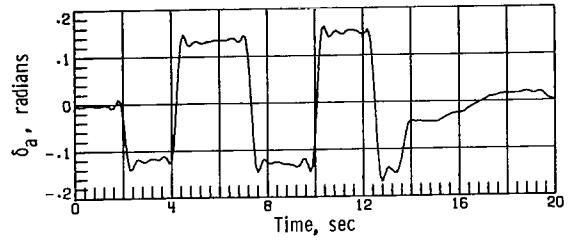


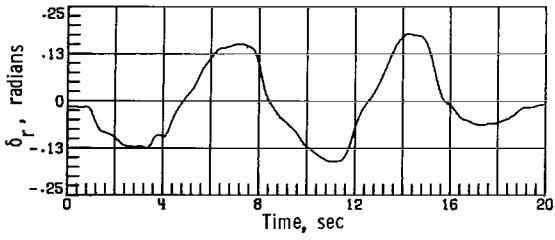
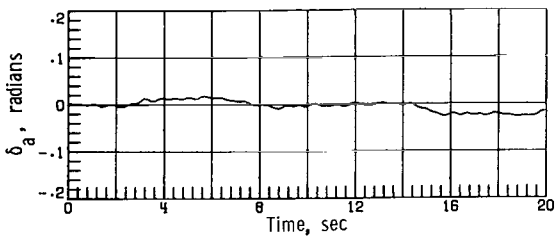
Figure 3.- Time histories of stabilator deflections illustrating the three longitudinal input forms used in this study.



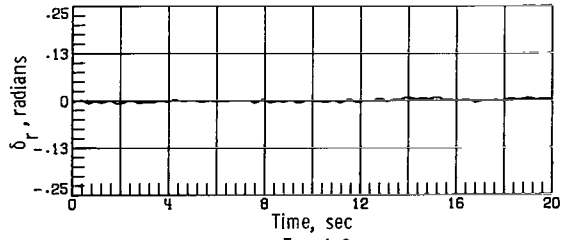
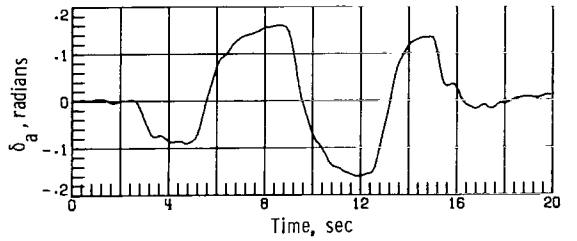
Input D



Input F



Input E



Input G

Figure 4.- Time histories illustrating the lateral control inputs used in this study.

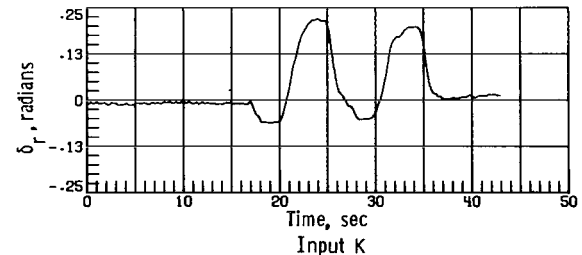
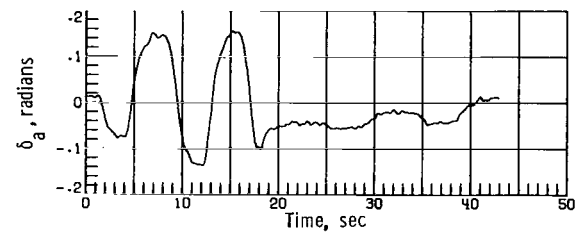
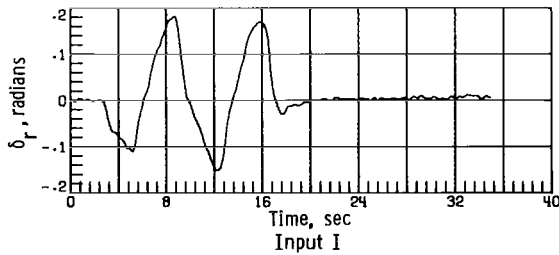
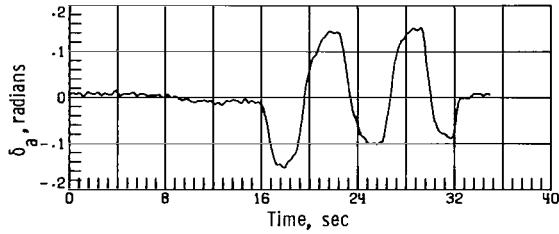
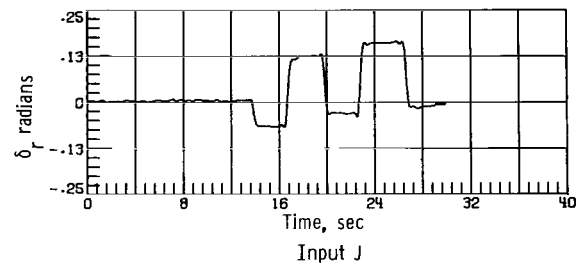
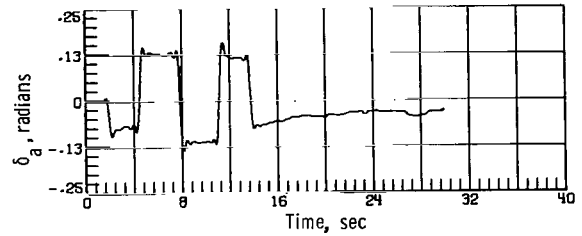
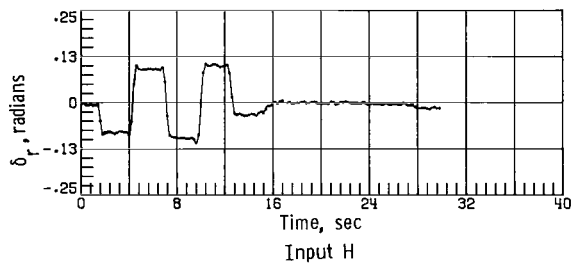
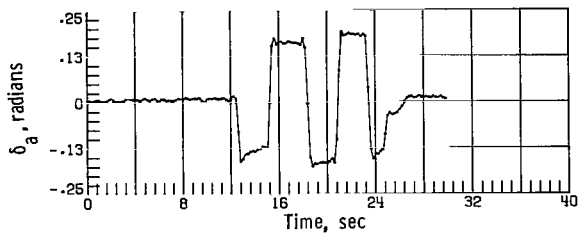


Figure 4.- Concluded.

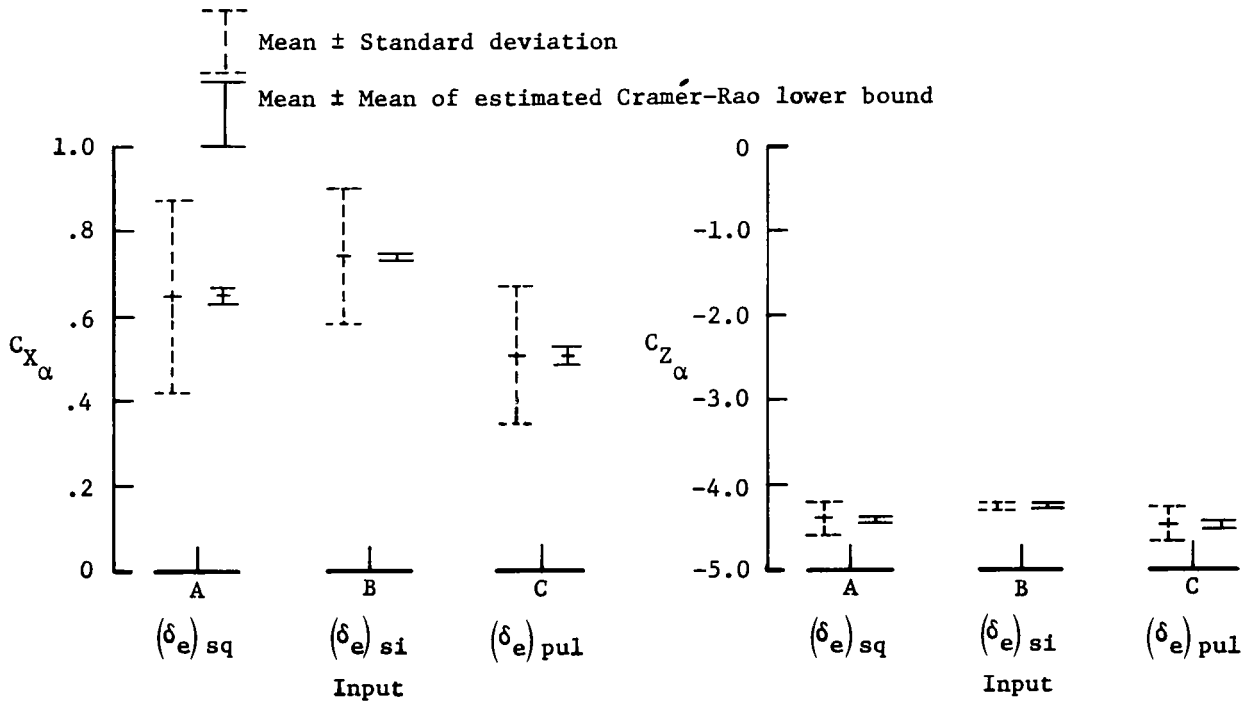
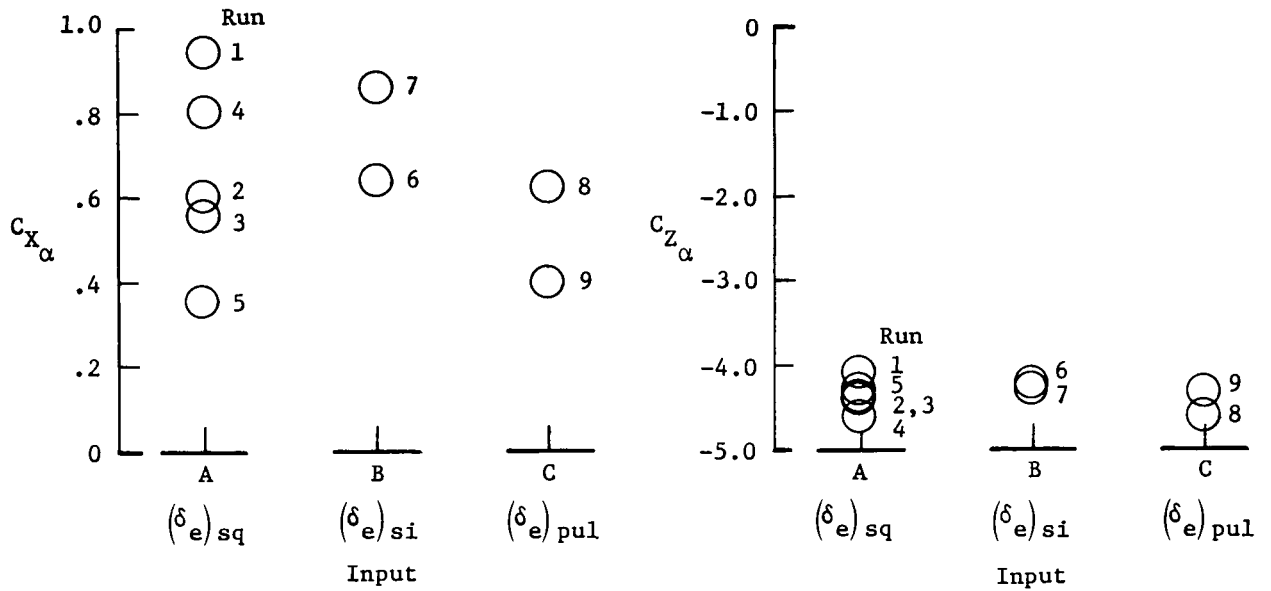


Figure 5.- Parameter values extracted for each longitudinal input along with corresponding run numbers and bars depicting ensemble variations and estimated Cramér-Rao lower bound on variations.

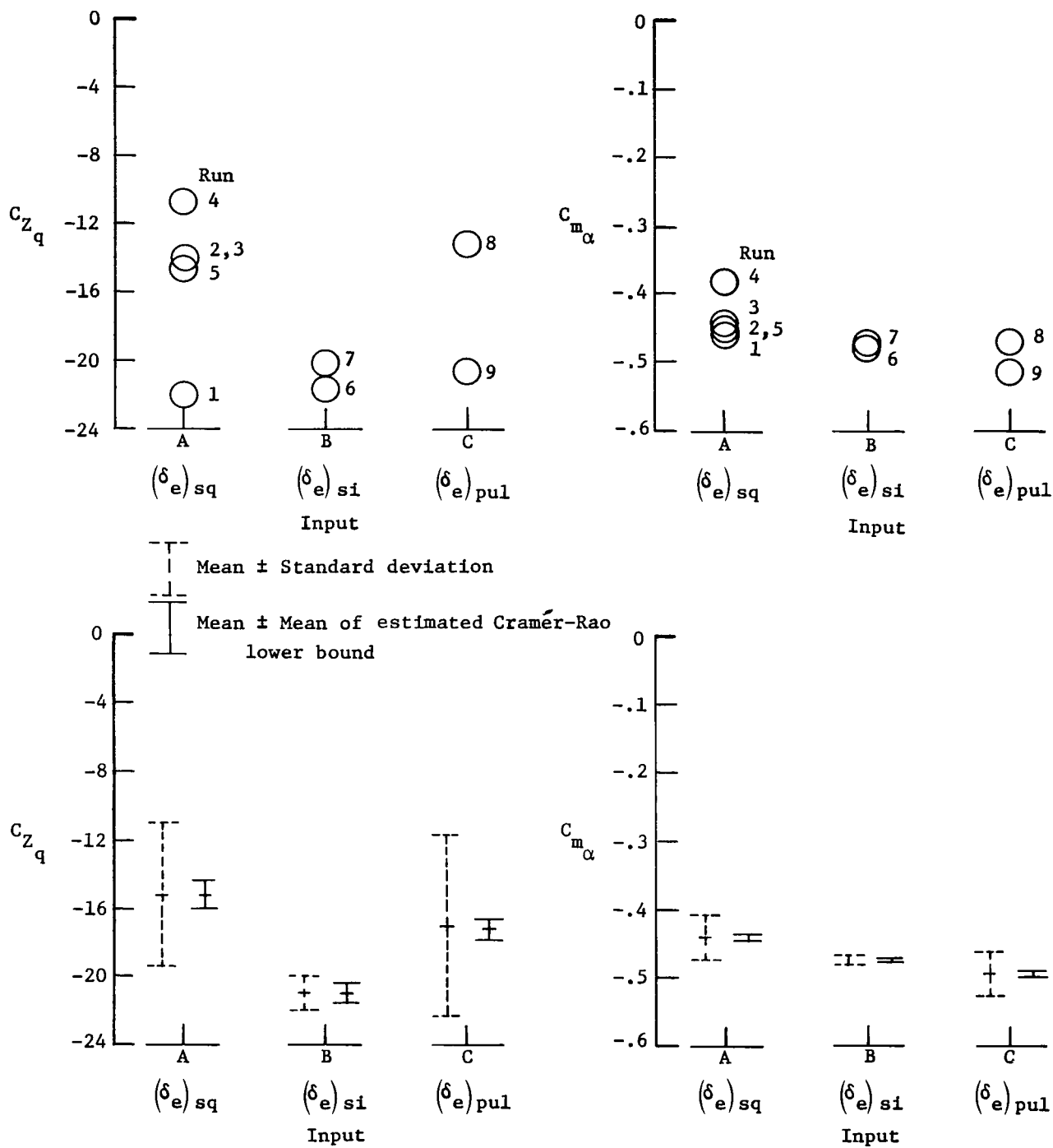


Figure 5.- Continued.

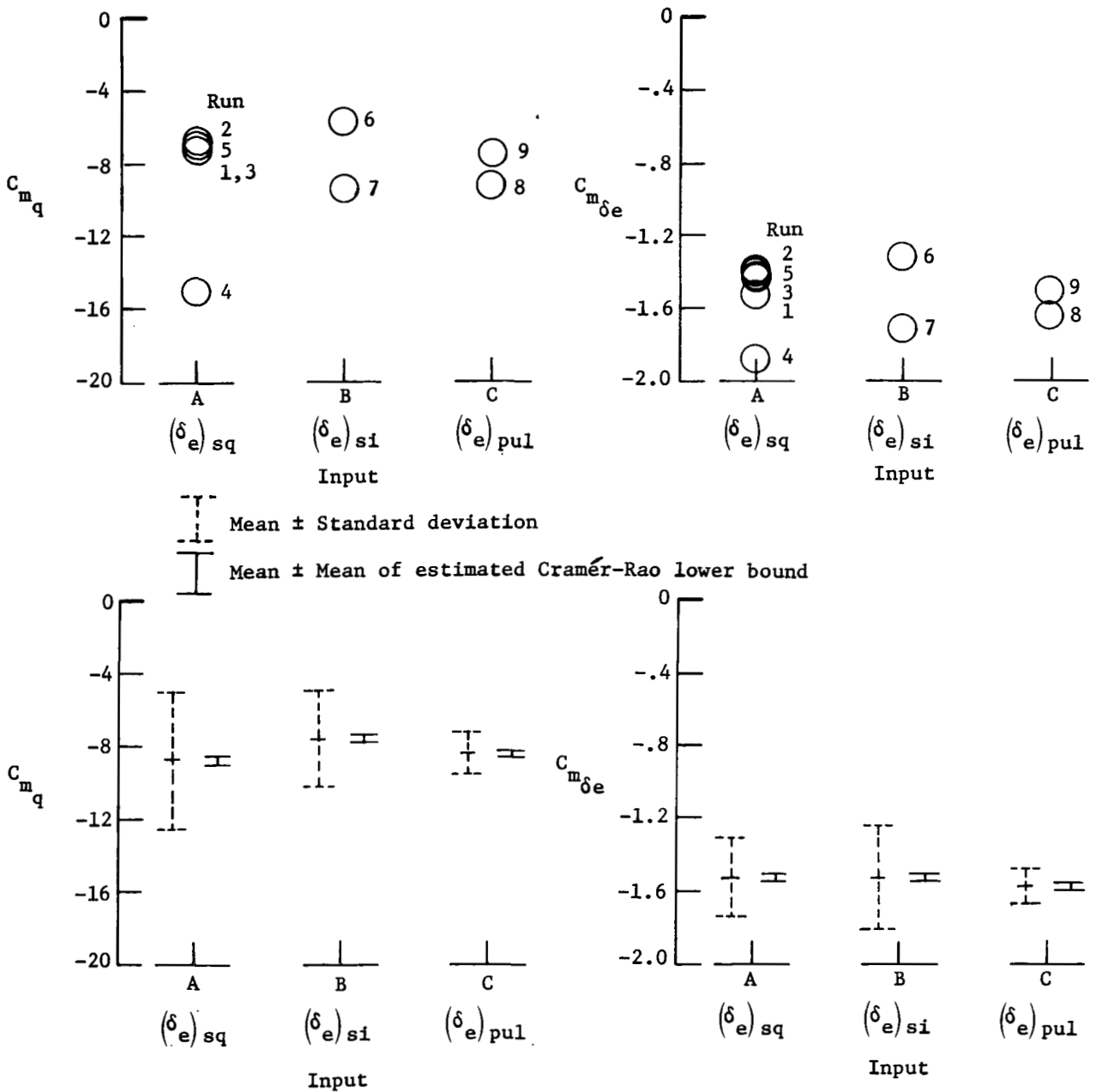


Figure 5.- Concluded.

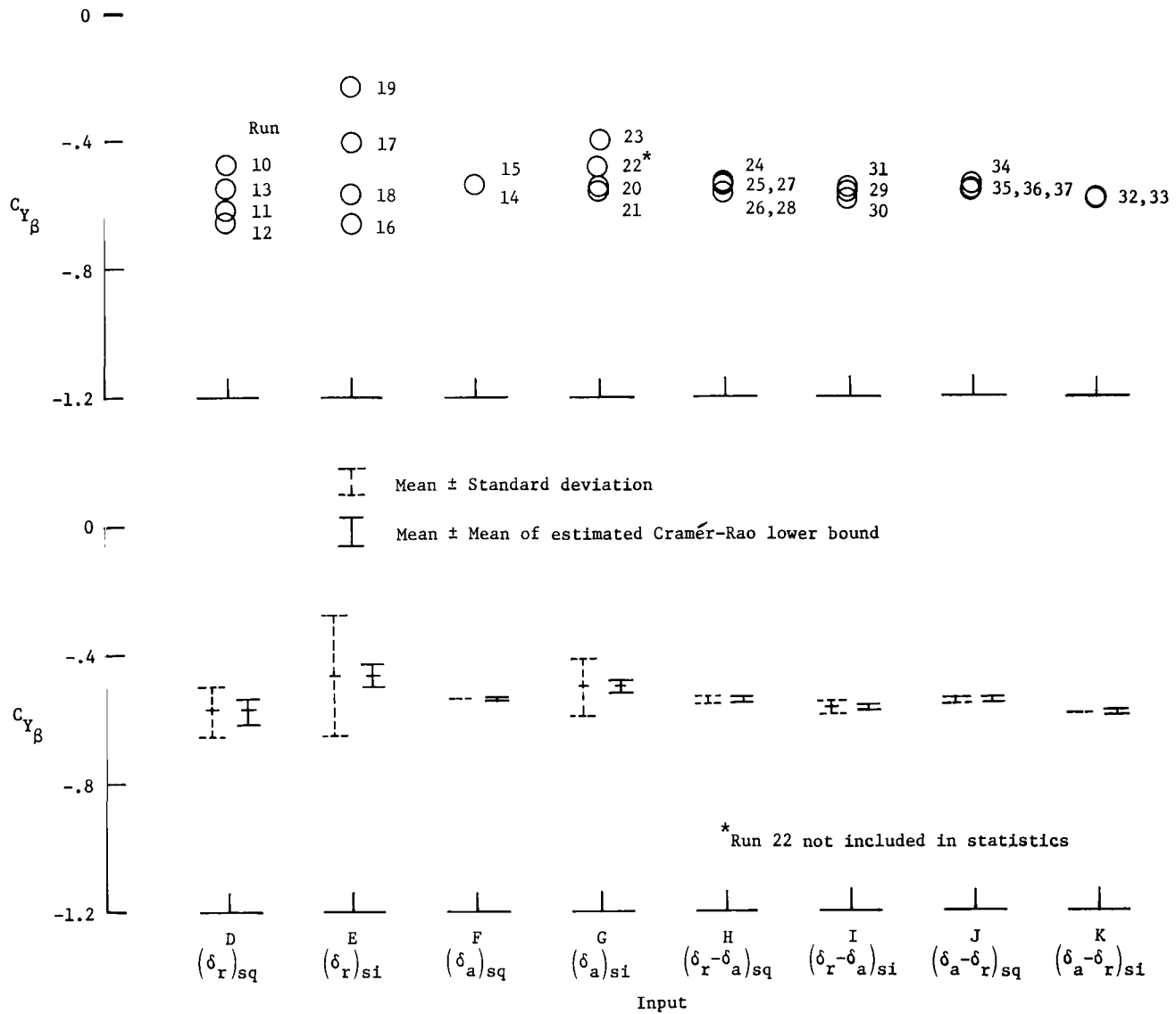


Figure 6.- Parameter values extracted for each lateral input along with the corresponding run numbers and bars depicting ensemble variations and estimated Cramér-Rao lower bound variations.

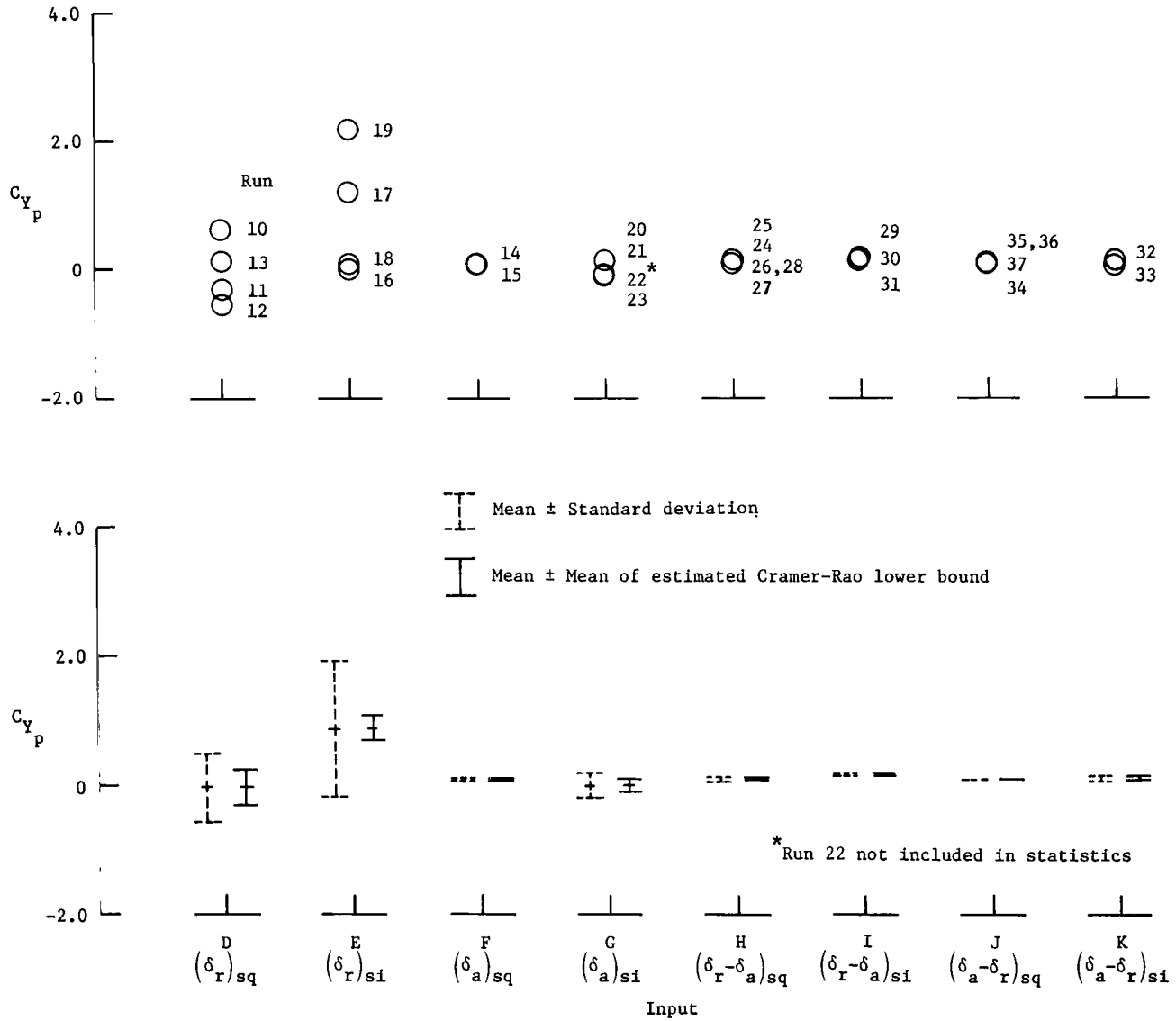


Figure 6.- Continued.

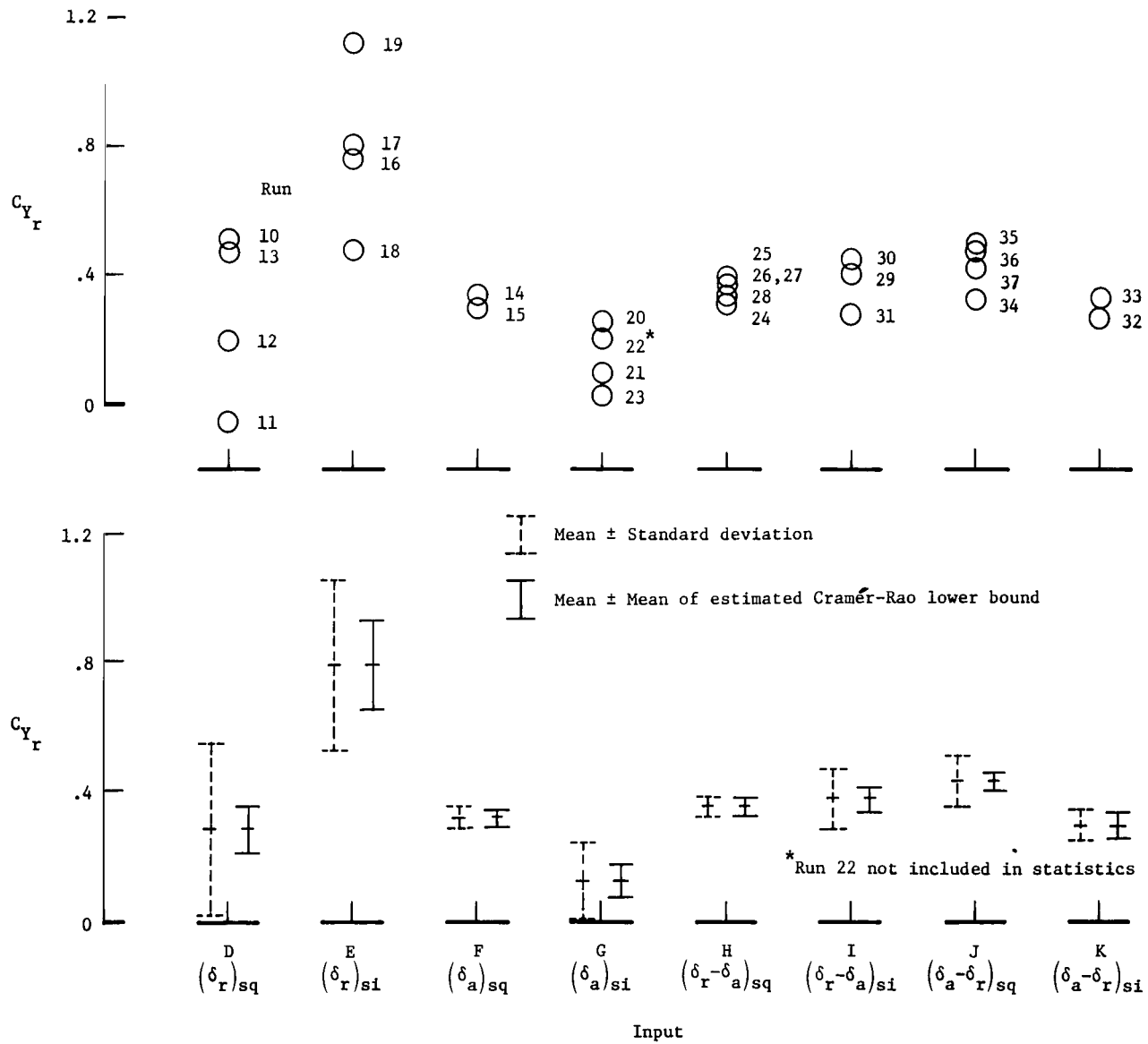


Figure 6.- Continued.

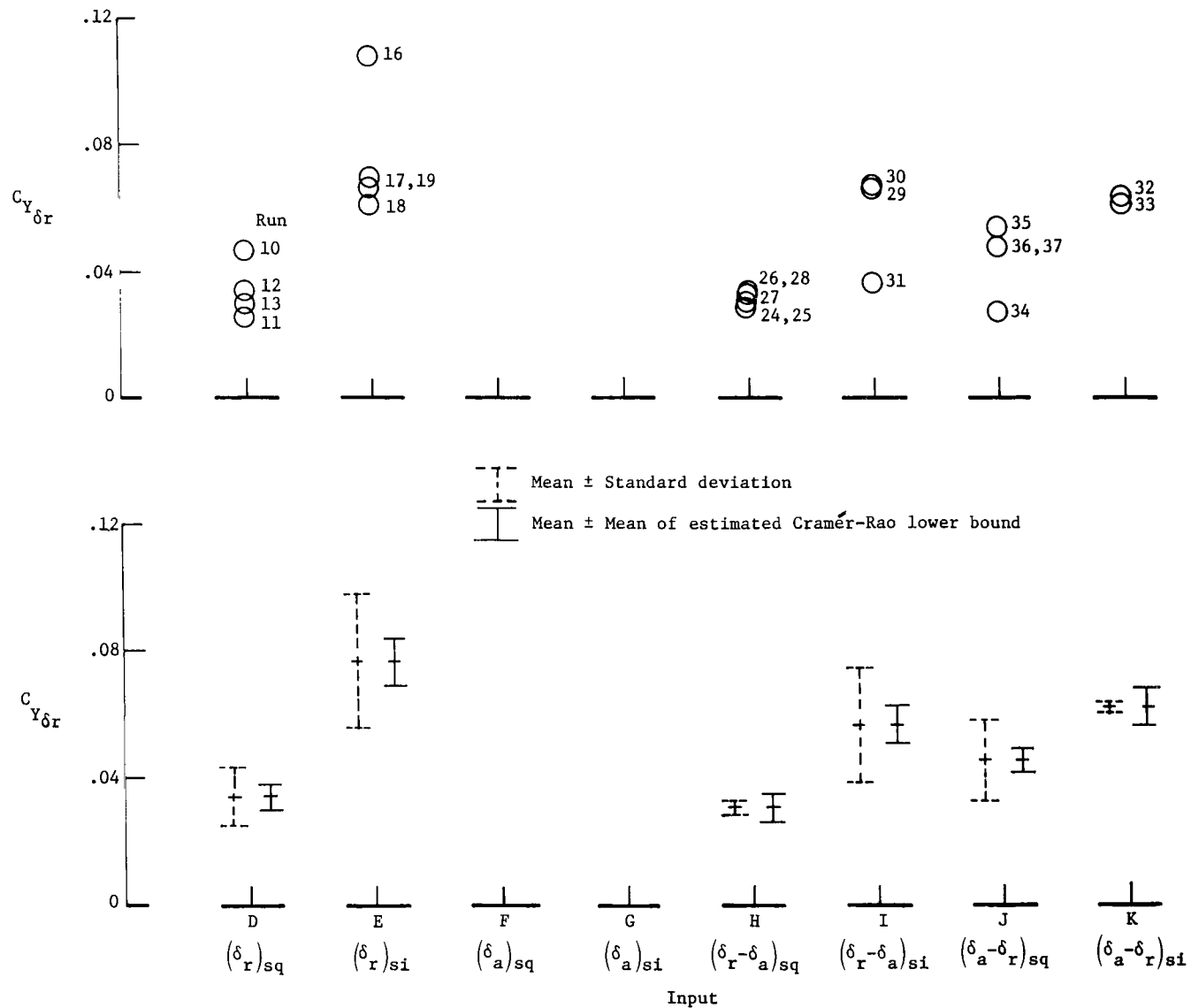


Figure 6.- Continued.

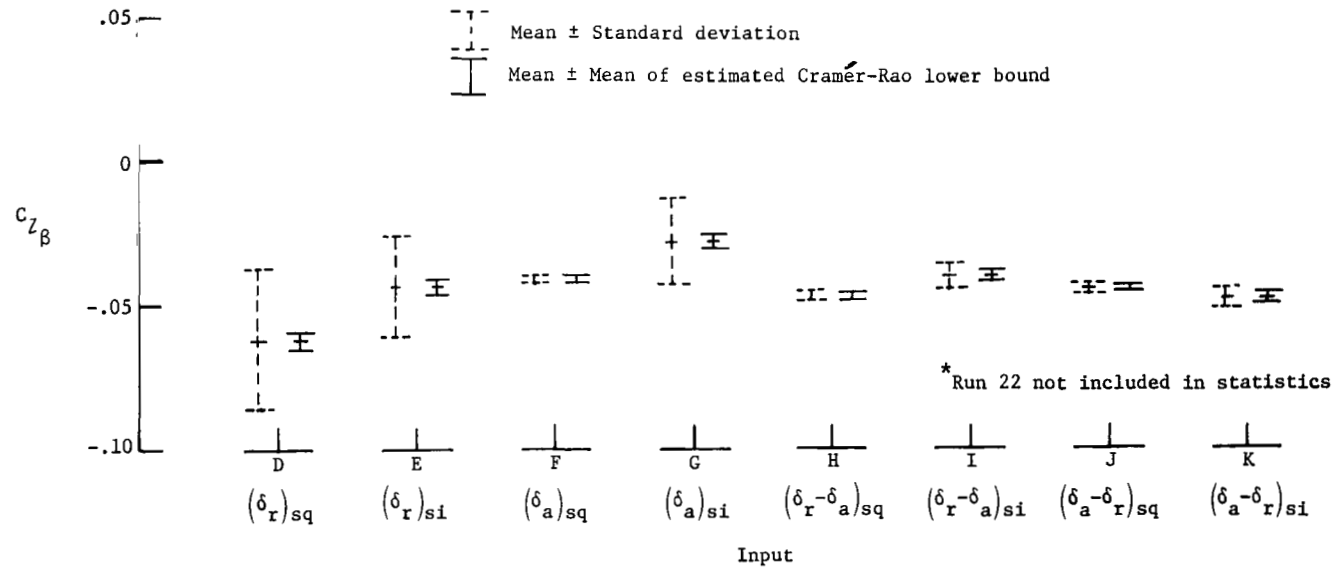
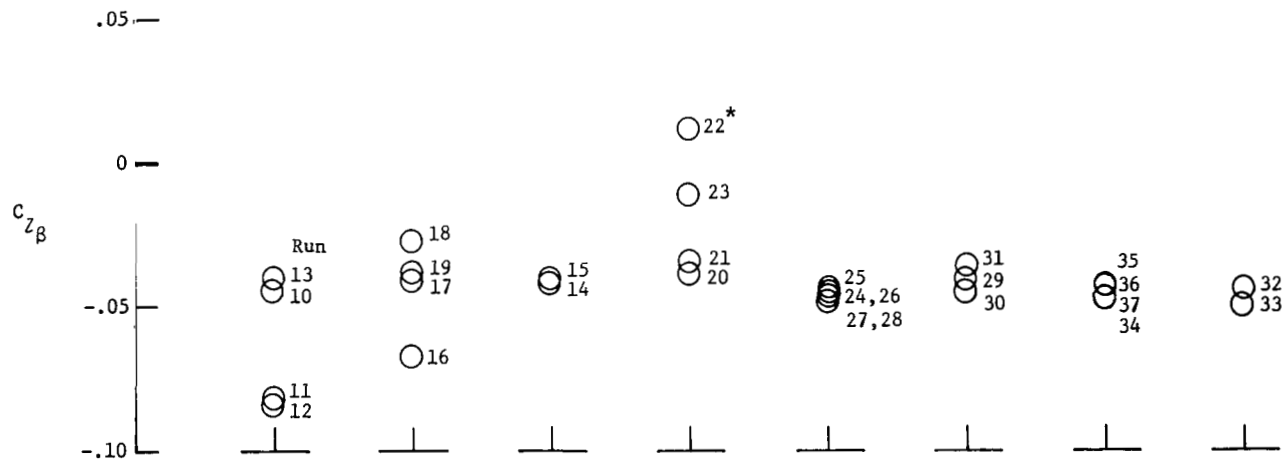


Figure 6.- Continued.

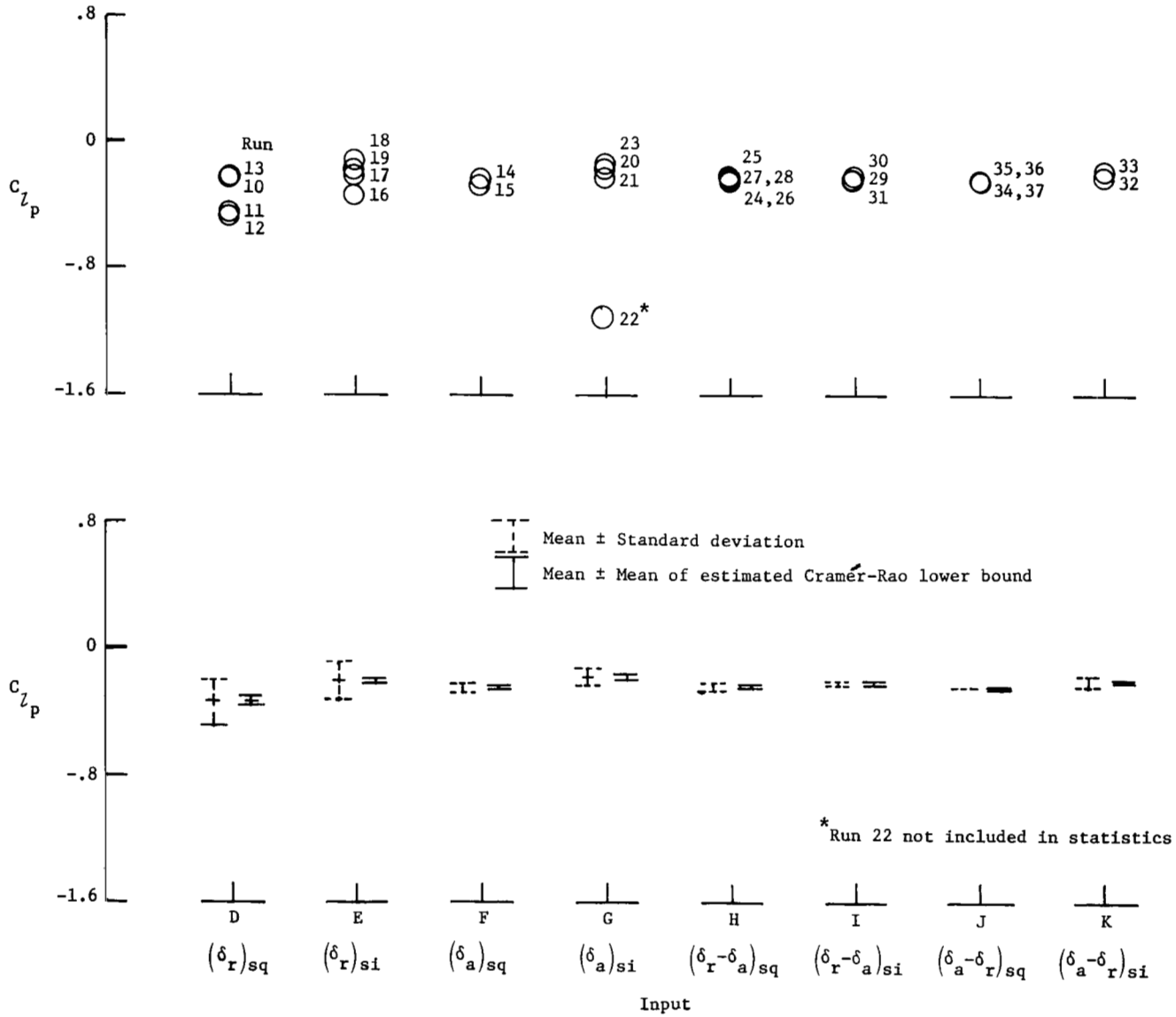


Figure 6.- Continued.

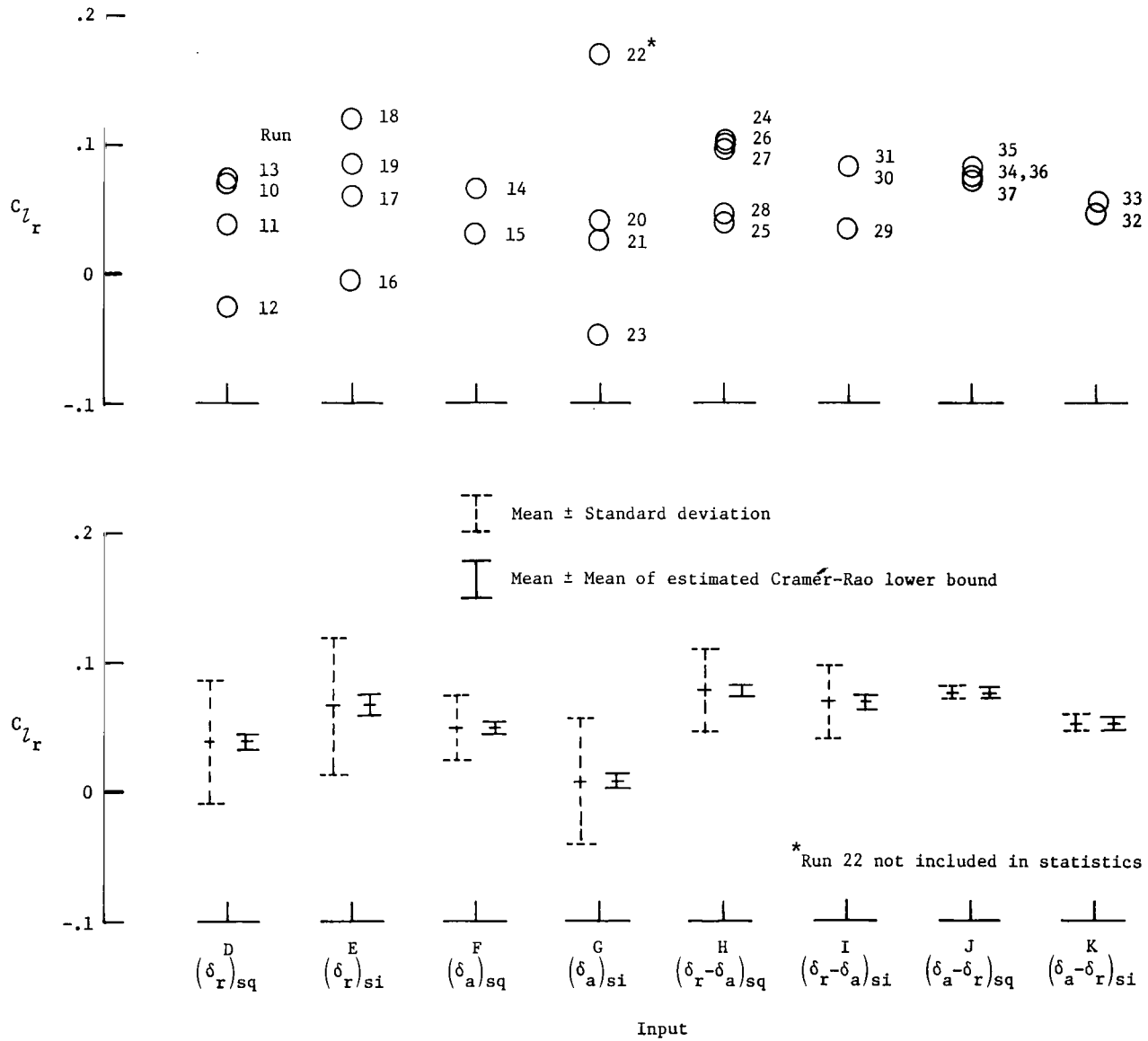


Figure 6.- Continued.

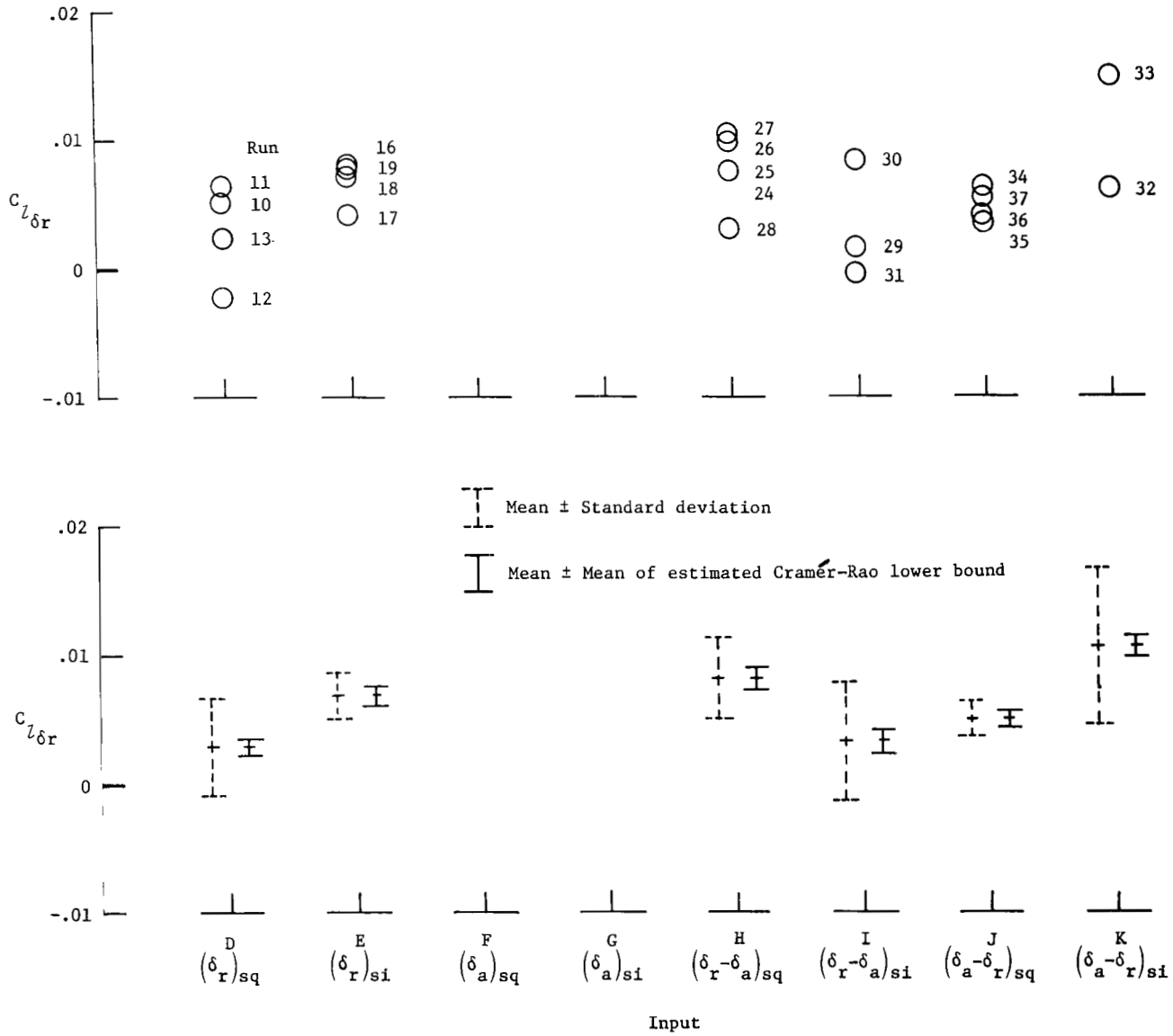


Figure 6.- Continued.

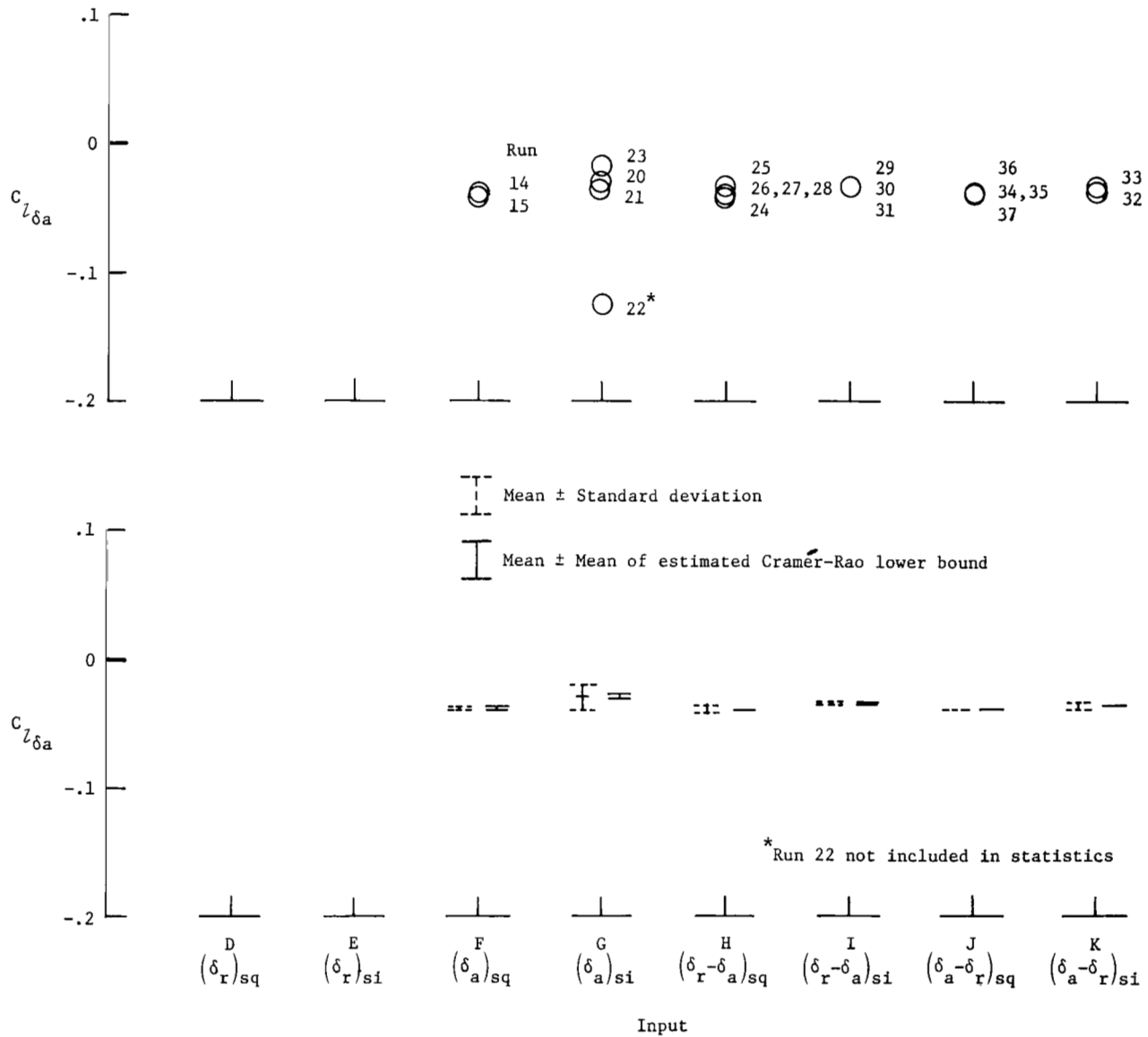


Figure 6.- Continued.

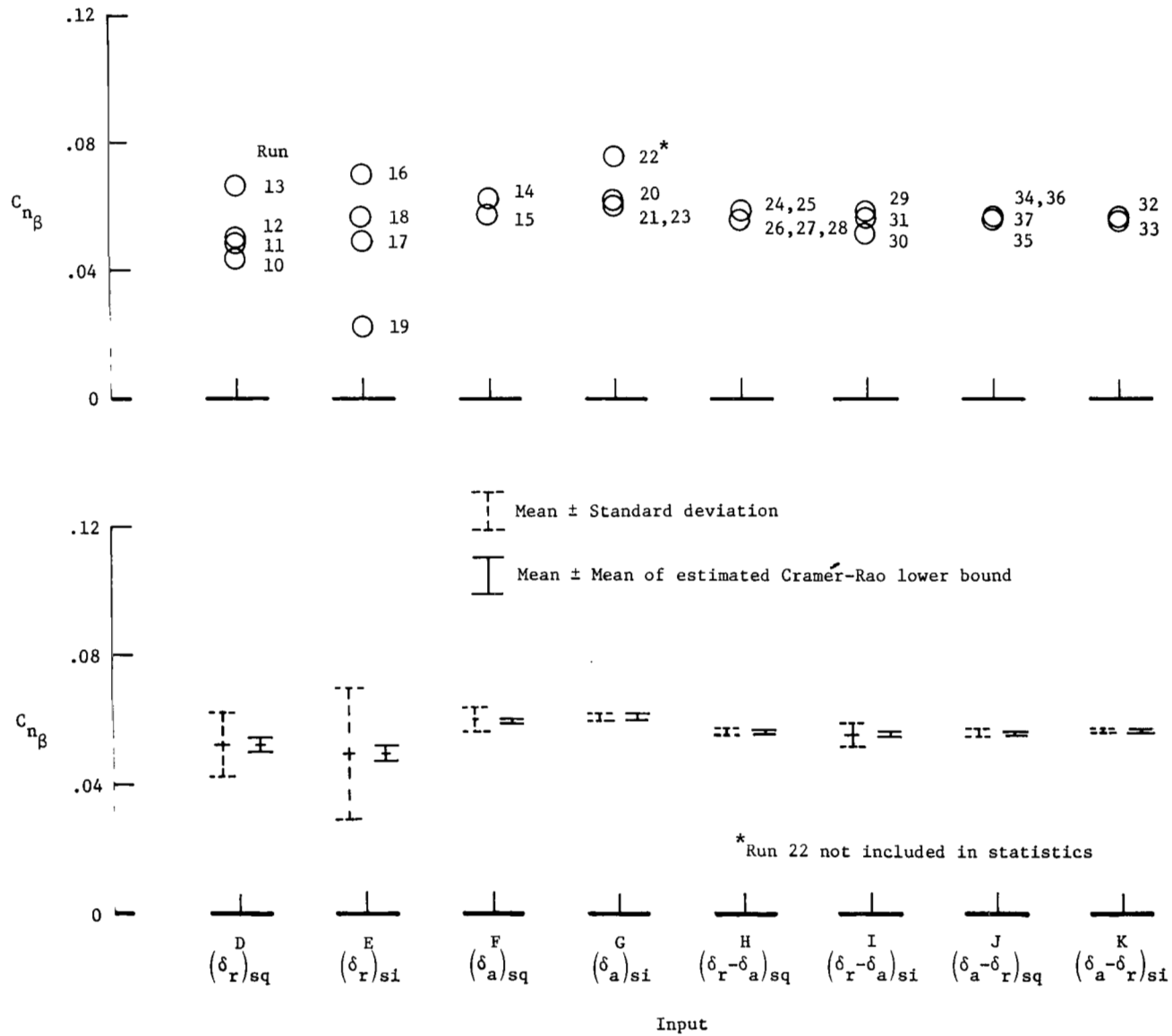


Figure 6.- Continued.

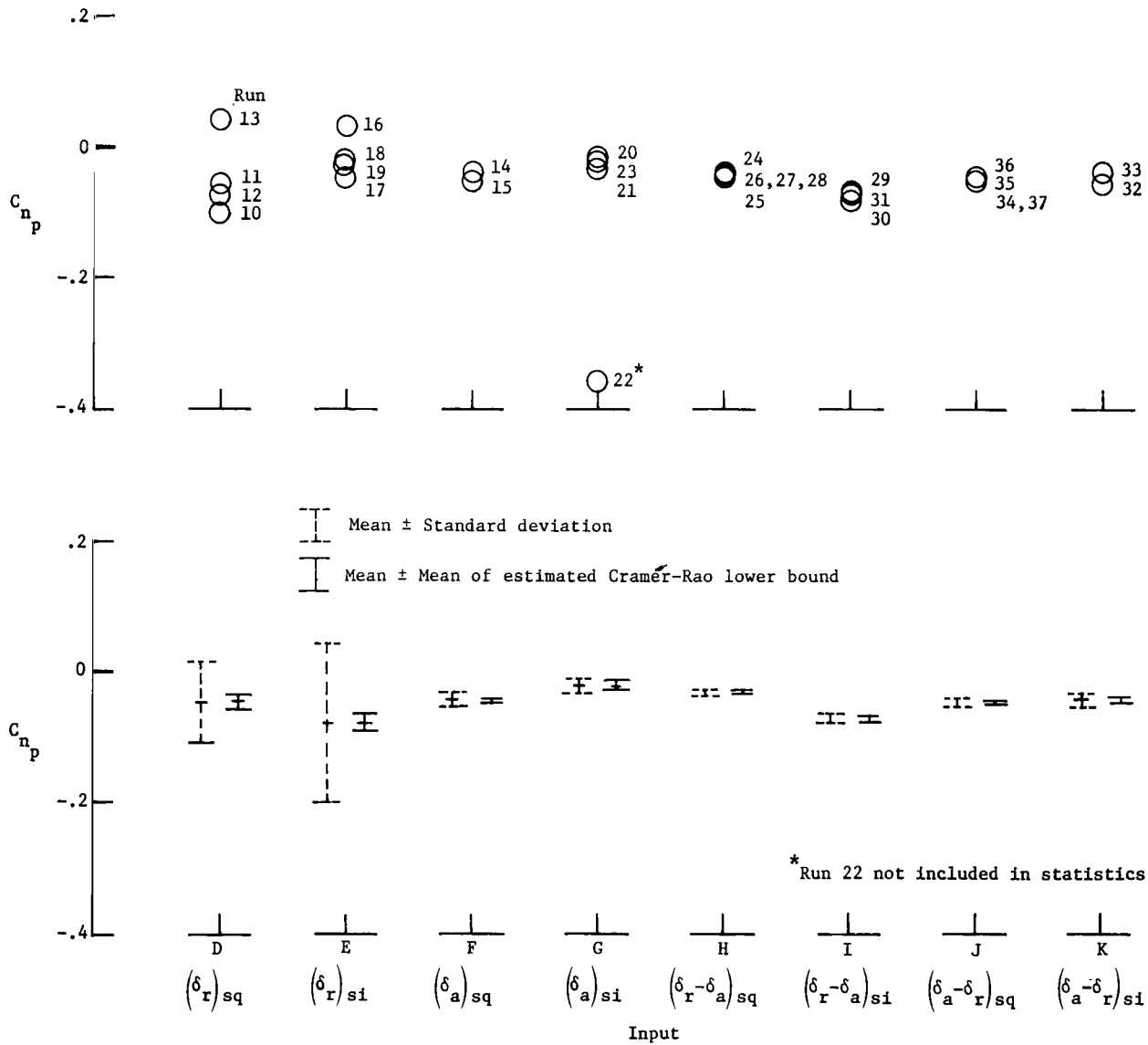


Figure 6.- Continued.

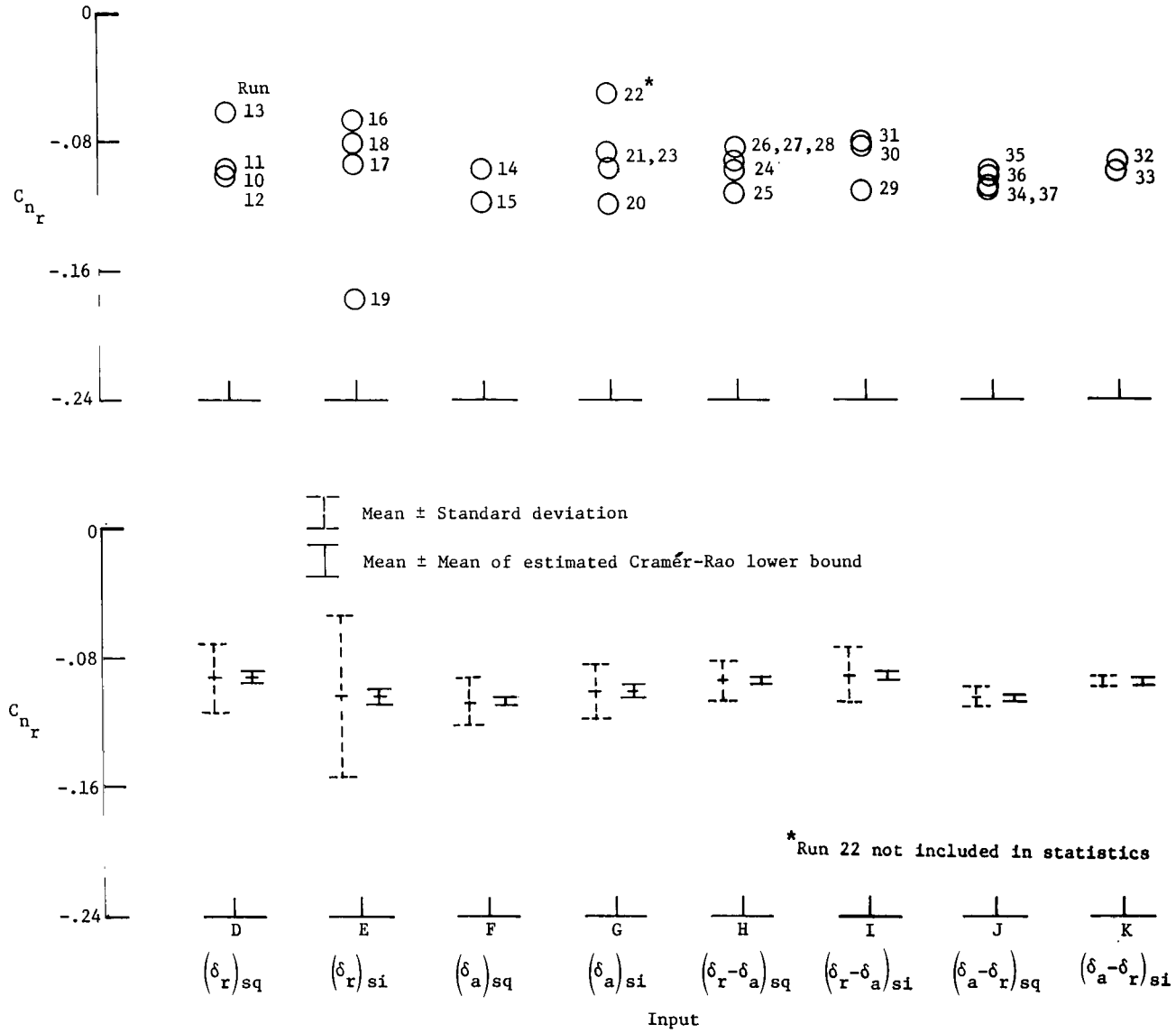


Figure 6.- Continued.

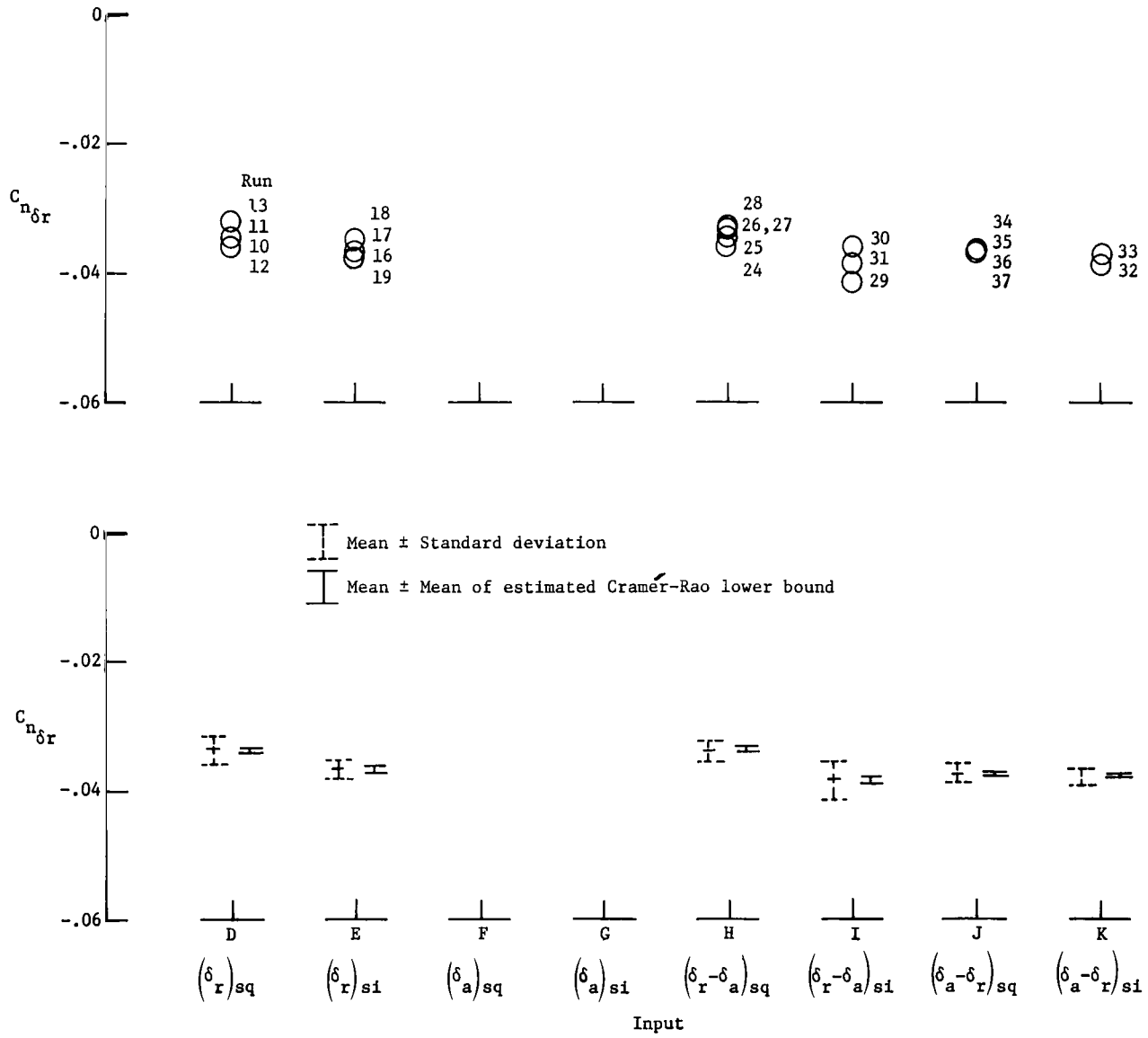


Figure 6.- Continued.

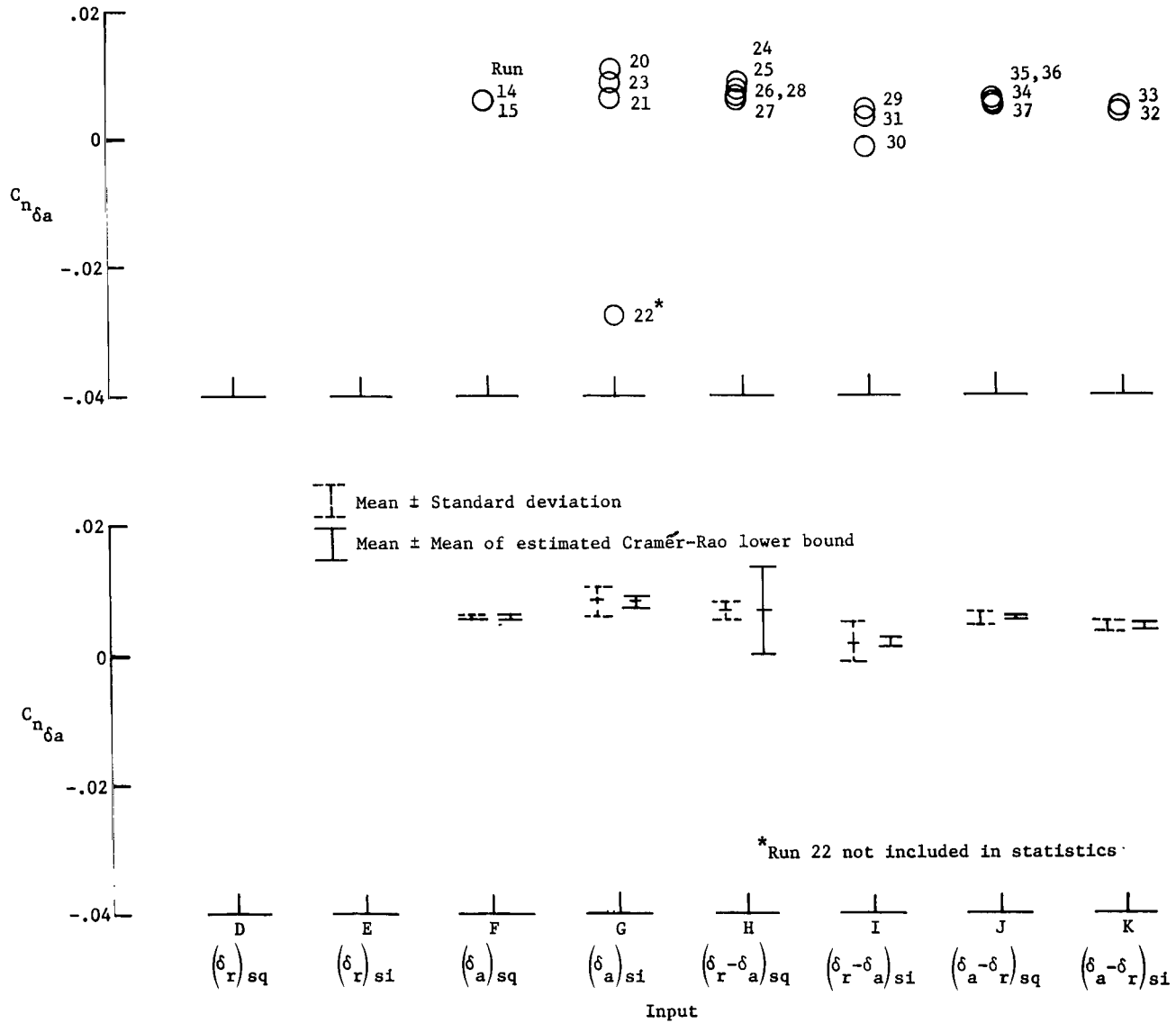


Figure 6.- Concluded.

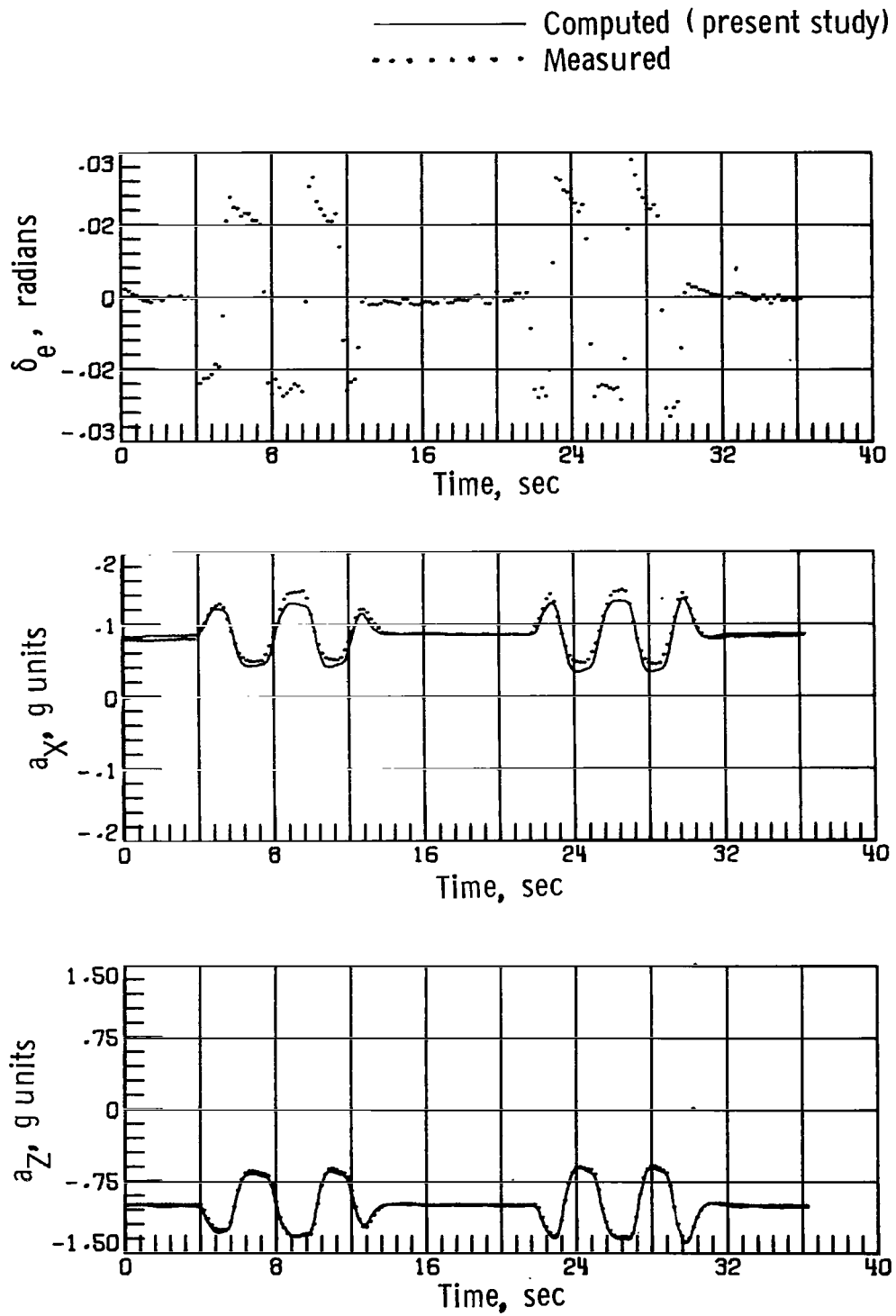


Figure 7.- Longitudinal control input and measured and computed responses to this input based on derivatives obtained in this study by use of maximum likelihood method and presented in table VI.

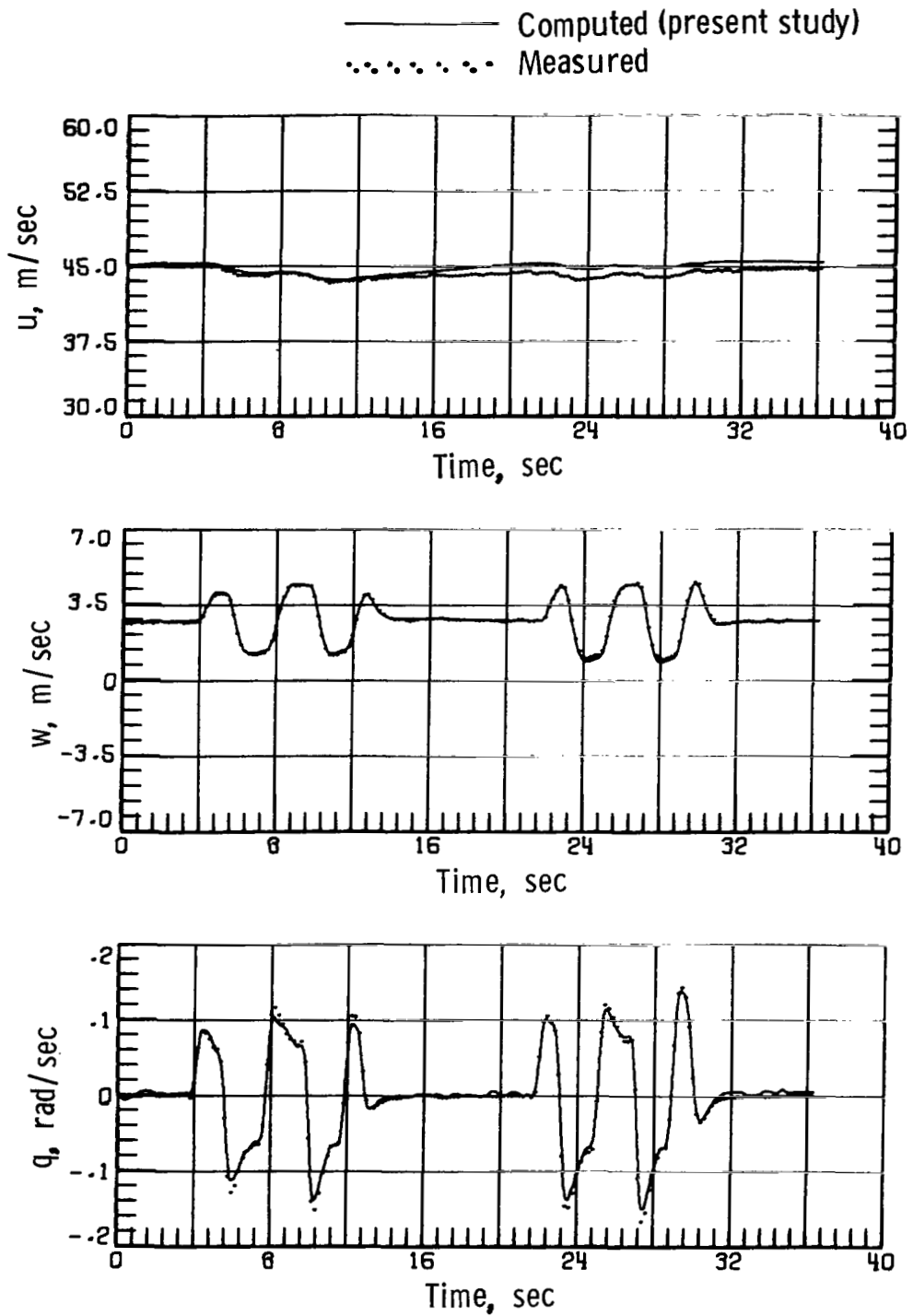


Figure 7.- Concluded.

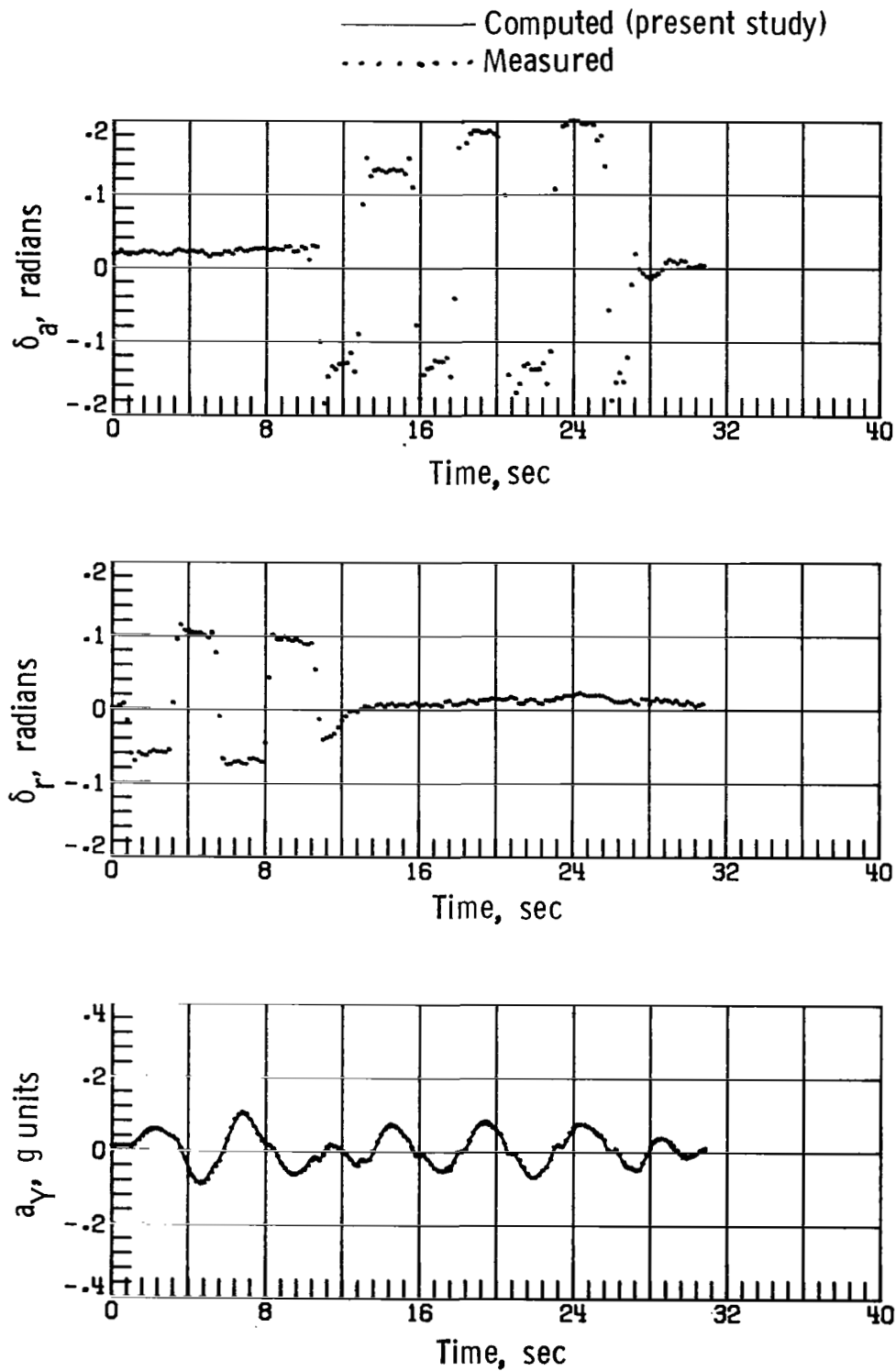


Figure 8.- Lateral control inputs and measured and computed responses to these inputs based on derivatives obtained in this study by use of maximum likelihood method and presented in table VI.

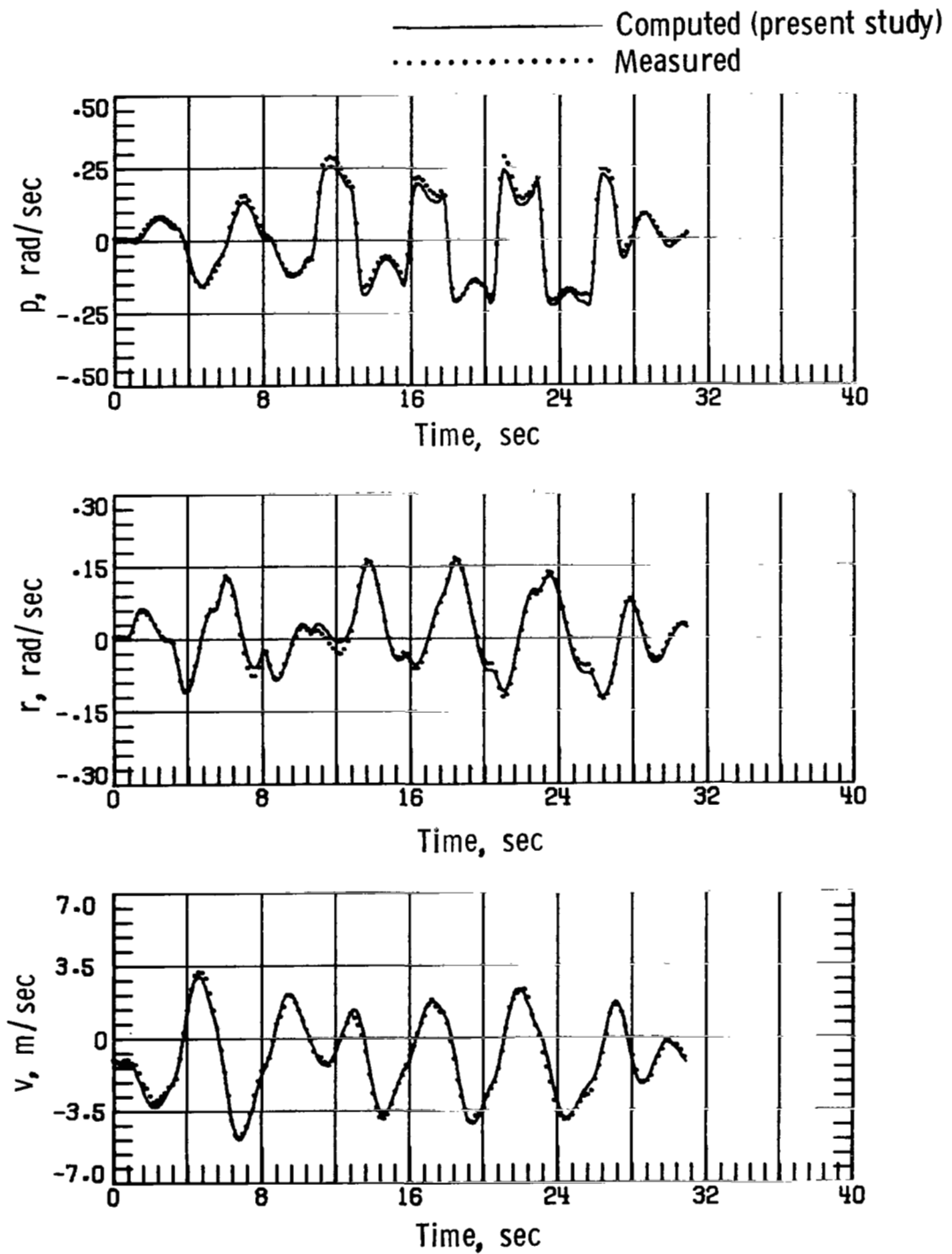


Figure 8.- Concluded.

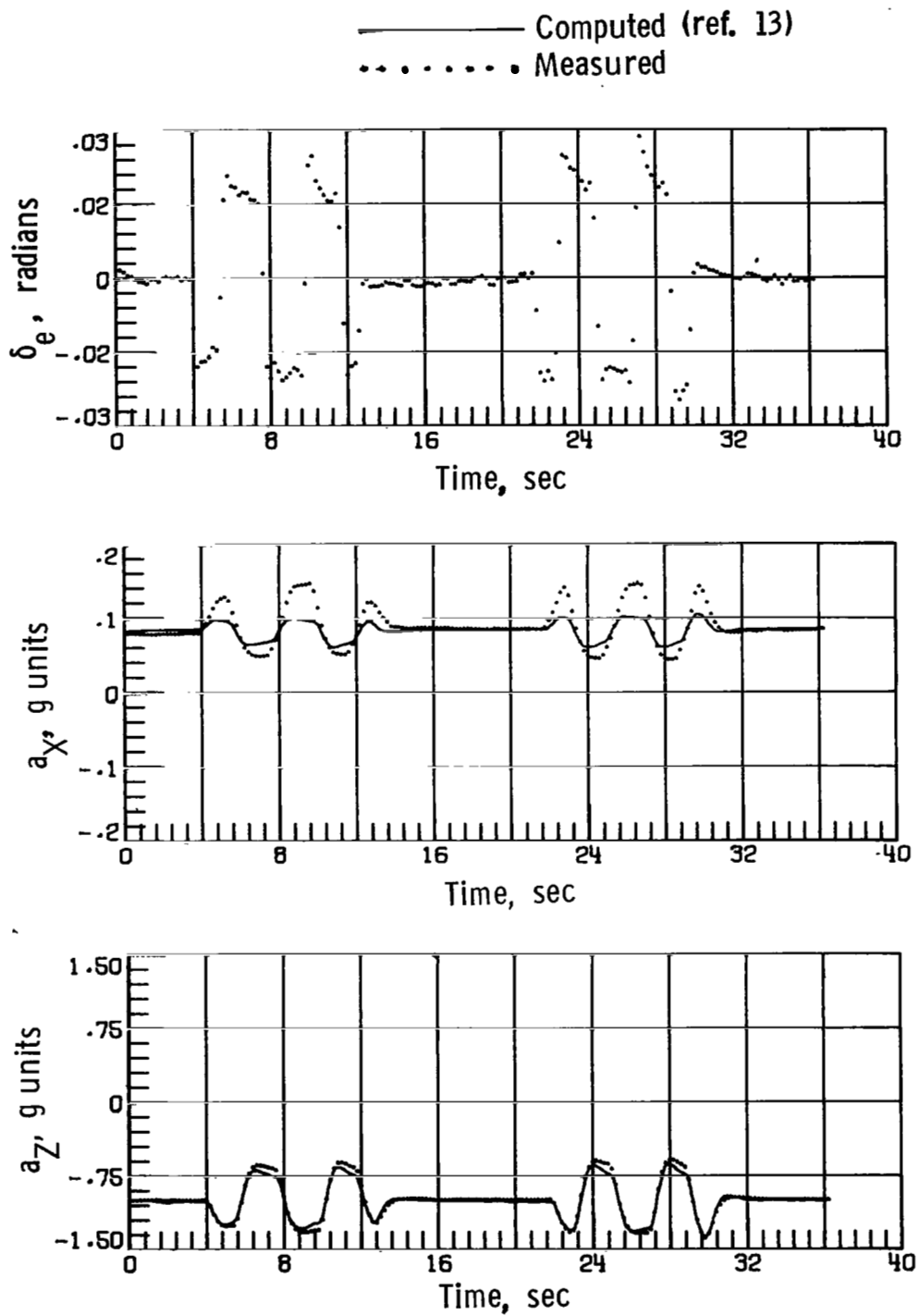


Figure 9.- Longitudinal flight data time histories and those computed by using derivatives obtained by methods of reference 13 and given in table VII.

———— Computed (ref. 13)
..... Measured

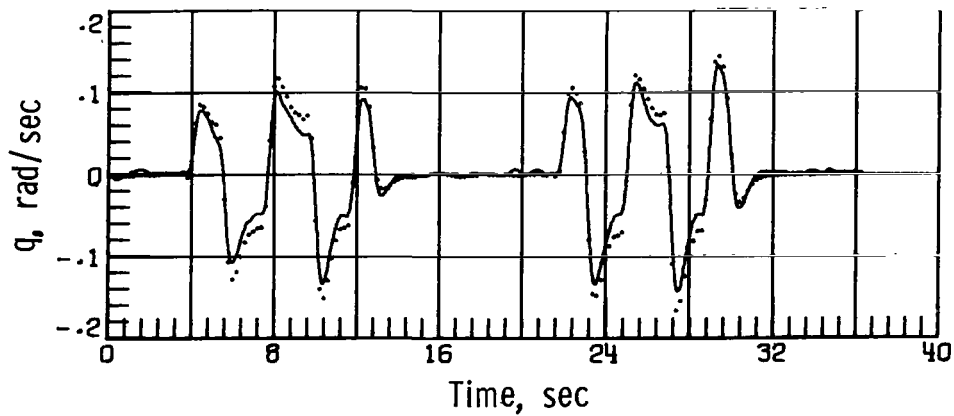
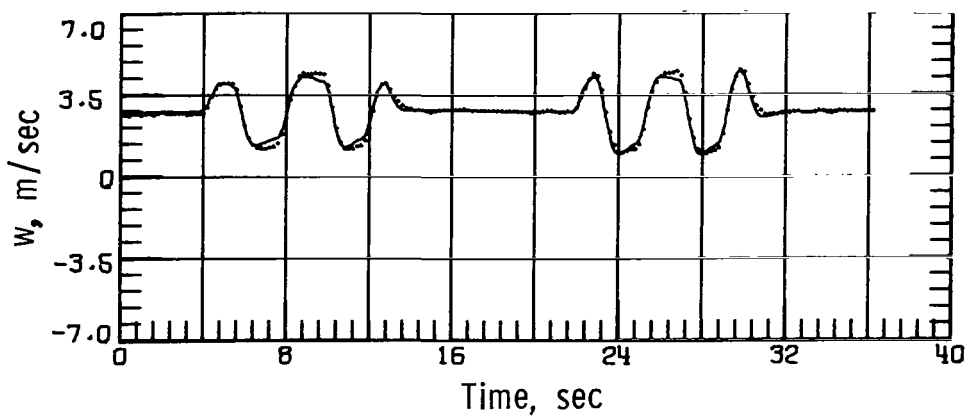
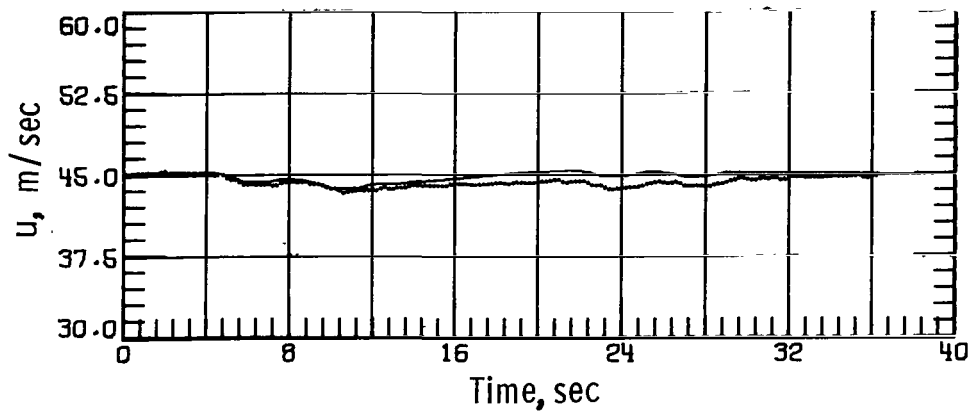


Figure 9.- Concluded.

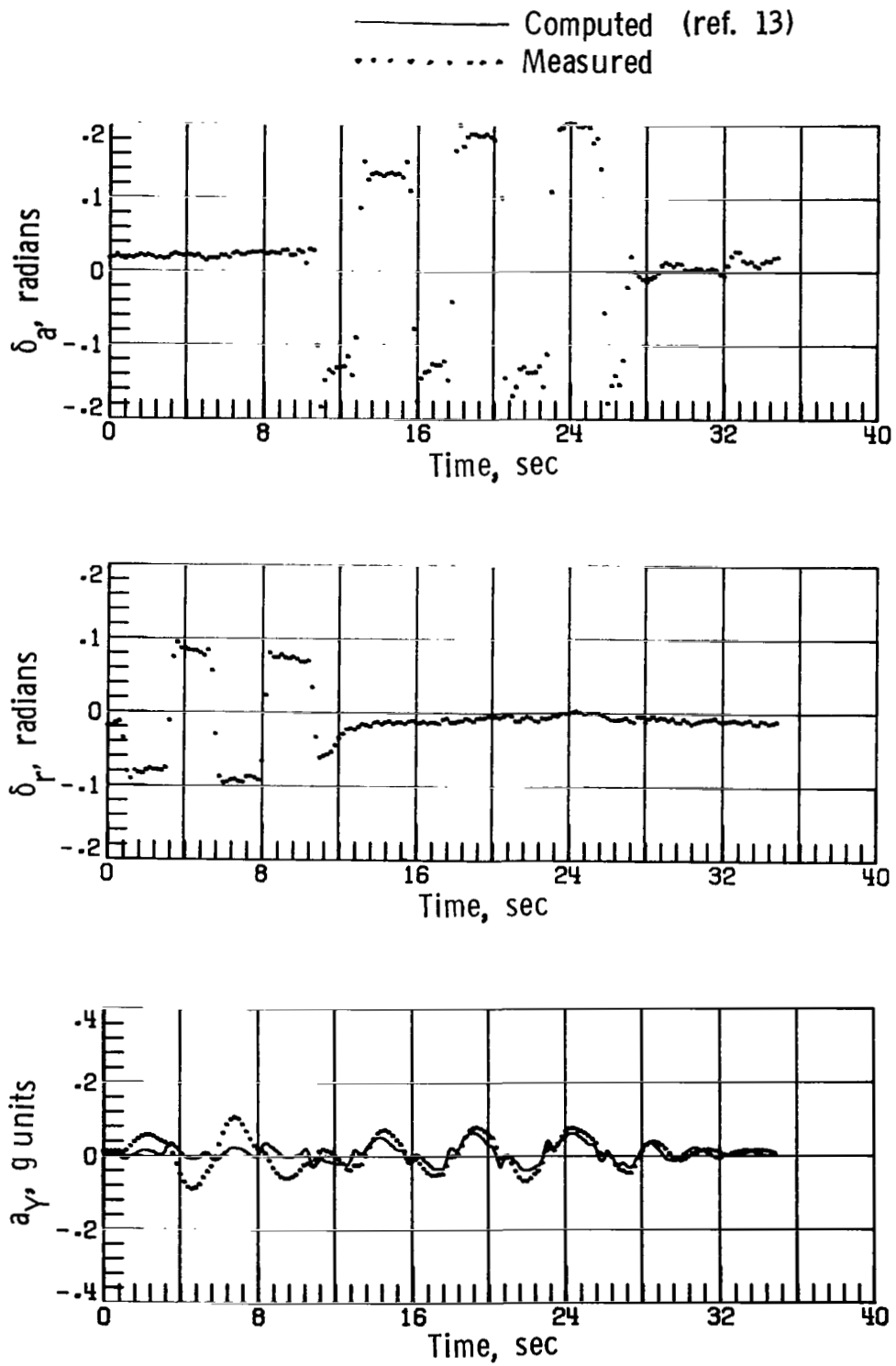


Figure 10.- Lateral flight data time histories and those computed by using derivatives obtained by methods of reference 13 and given in table VII.

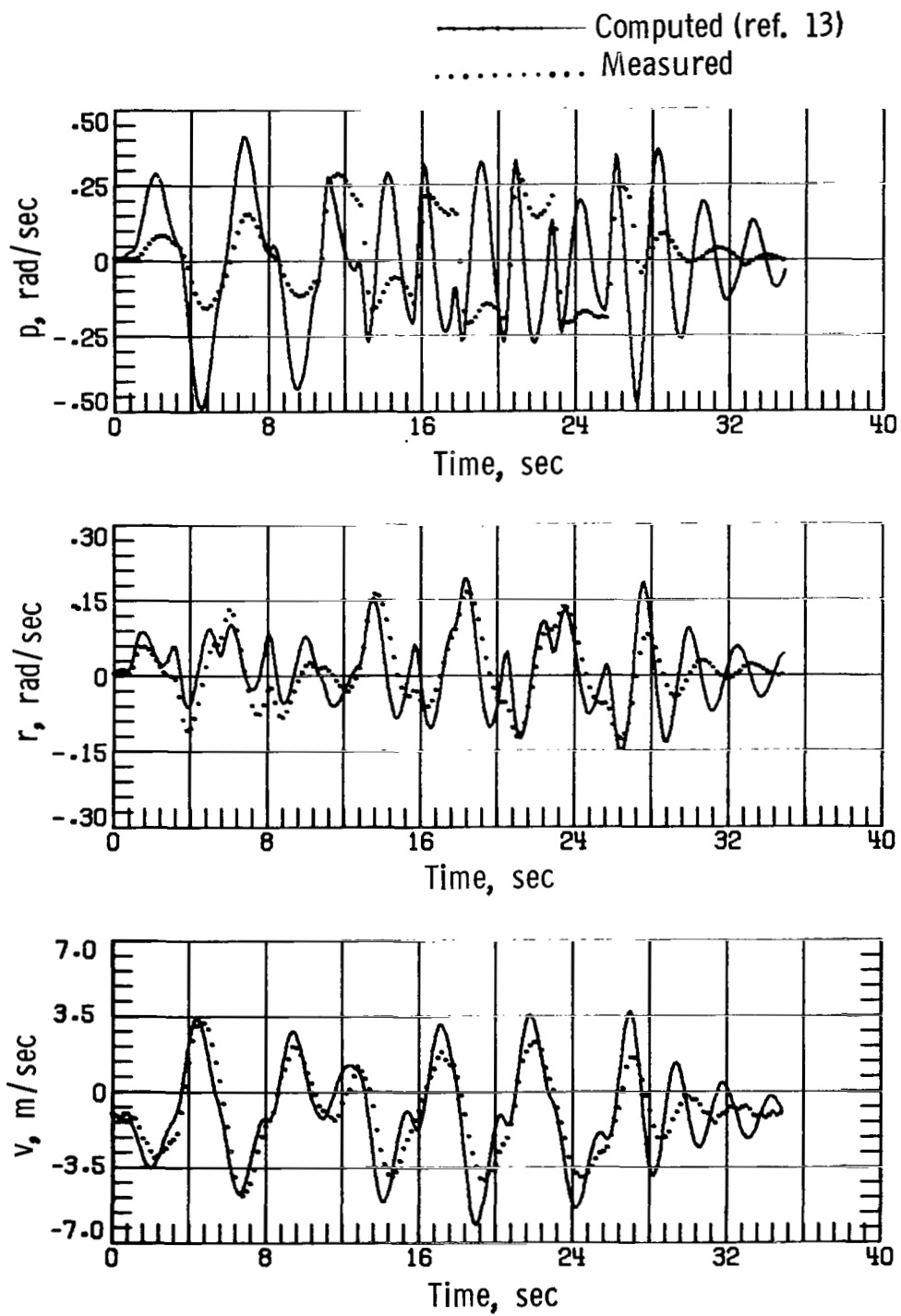


Figure 10.- Concluded.

1. Report No. NASA TP-1043		2. Government Accession No.		3. Recipient's Catalog No.	
4. Title and Subtitle EFFECTS OF CONTROL INPUTS ON THE ESTIMATION OF STABILITY AND CONTROL PARAMETERS OF A LIGHT AIRPLANE				5. Report Date December 1977	
7. Author(s) Robert L. Cannaday and William T. Suit				6. Performing Organization Code	
9. Performing Organization Name and Address NASA Langley Research Center Hampton, VA 23665				8. Performing Organization Report No. L-11355	
12. Sponsoring Agency Name and Address National Aeronautics and Space Administration Washington, DC 20546				10. Work Unit No. 505-10-11-01	
15. Supplementary Notes				11. Contract or Grant No.	
16. Abstract <p>The maximum likelihood parameter estimation technique was used to determine the values of stability and control derivatives from flight test data for a low-wing, single-engine, light airplane. Several input forms were used during the tests to investigate the consistency of parameter estimates as it relates to inputs. These consistencies were compared by using the ensemble variance and estimated Cramér-Rao lower bound. In addition, the relationship between inputs and parameter correlations was investigated. Results from the stabilator inputs are inconclusive but the sequence of rudder input followed by aileron input or aileron followed by rudder gave more consistent estimates than did rudder or ailerons individually. Also, square-wave inputs appeared to provide slightly improved consistency in the parameter estimates when compared to sine-wave inputs.</p>				13. Type of Report and Period Covered Technical Paper	
17. Key Words (Suggested by Author(s)) Parameter extraction Aerodynamic parameters Light aircraft Control inputs				14. Sponsoring Agency Code	
18. Distribution Statement Unclassified - Unlimited				Subject Category 08	
19. Security Classif. (of this report) Unclassified		20. Security Classif. (of this page) Unclassified		21. No. of Pages 70	
				22. Price \$5.25	

National Aeronautics and
Space Administration

Washington, D.C.
20546

Official Business
Penalty for Private Use, \$300

THIRD-CLASS BULK RATE

Postage and Fees Paid
National Aeronautics and
Space Administration
NASA-451



4 1 U.A. 120577 S00903DS
DEPT OF THE AIR FORCE
AF WEAPONS LABORATORY
ATTN: TECHNICAL LIBRARY (SUL)
KIRTLAND AFB NM 87117

NASA

S

POSTMASTER: If Undeliverable (Section 158
Postal Manual) Do Not Return
